

# **Structural and Thermodynamic Investigation of Iodide Uptake by Pyrite and Layered Double Hydroxides**

Inauguraldissertation  
der Philosophisch-naturwissenschaftlichen Fakultät  
der Universität Bern

vorgelegt von  
**Laure Aimoz**  
von Frankreich

Leiter der Arbeit: PD Dr. U. Mäder (Institut für Geologie)  
Co-Leiter: Dr. E. Curti (Paul Scherrer Institut)  
Co-Leiter: Dr. E. Wieland (Paul Scherrer Institut)  
Co-Leiterin: Dr. C. Taviot-Guého (Institut de Chimie de Clermont-Ferrand)  
Koreferent: Dr. A. Scheinost (European Synchrotron Radiation Facility)



# **Structural and Thermodynamic Investigation of Iodide Uptake by Pyrite and Layered Double Hydroxides**

Inauguraldissertation  
der Philosophisch-naturwissenschaftlichen Fakultät  
der Universität Bern

vorgelegt von  
**Laure Aimoz**  
von Frankreich

Leiter der Arbeit: PD Dr. U. Mäder (Institut für Geologie)  
Co-Leiter: Dr. E. Curti (Paul Scherrer Institut)  
Co-Leiter: Dr. E. Wieland (Paul Scherrer Institut)  
Co-Leiterin: Dr. C. Taviot-Guého (Institut de Chimie de Clermont-Ferrand)  
Koreferent: Dr. A. Scheinost (European Synchrotron Radiation Facility)

Von der Philosophisch-naturwissenschaftlichen Fakultät angenommen.

Bern, den 27. April 2012

Der Dekan:  
Prof. Dr. Silvio Decurtins

## **Acknowledgments**

### **Financial supports:**

The Helmholtz virtual institute of advanced solid-aqueous radiogeochemistry, the Swiss cooperative for the disposal of radioactive waste (Nagra), and PSI are greatly acknowledged.

### **This PhD thesis benefited from the professional contribution of many people:**

Dr. Urs Mäder is thanked for dealing with the non-rewarding paperwork, for sharing interest in this scientific work, and for his nice support that always kept my motivation up.

Dr. Enzo Curti is thanked for initiating this project, for giving me the freedom to choose the directions I wanted to follow, and for his kind patience to adapt to my demanding wishes.

Dr. Erich Wieland is thanked for his educational and mentoring attitude, and for his ability to give me good feedbacks during my work advancements.

Dr. Christine Taviot-Guého is thanked for her great participation in this work and for her excellent ability to transfer scientific knowledge, even 600 km away.

Dr. Andreas Scheinost is thanked for accepting to be the external adviser of this PhD work and for his effective support with the EXAFS data analysis.

Dr. Sergey Churakov is thanked for helping me to understand my minerals and for accepting to lately, but very efficiently, jump in this project.

Dr. Dmitrii Kulik is thanked for his excitement on the thermodynamic modeling part of my work and for his implication to make it successful.

Dr. Barbara Lothenbach is thanked for her never-ending enthusiasm, and for sharing unconditionally her tips and tricks on synthesis and modeling.

Dr. Urs Berner is thanked for great discussions on cement chemistry and on radioactive waste in general, and for his permanent diplomatic support.

## *Acknowledgments*

---

Dr. Rainer Dähn and Dr. Marika Vespa are thanked for joining the EXAFS beamtime in Grenoble and for supervising the related work.

Dr. Martin Glaus and Werner Müller are greatly acknowledged for the ion chromatography measurements and for always aiming at increasing accuracy and precision.

All members of the rock-water interaction group are warmly thanked for their welcome during my several journeys at the Institute of Geological Sciences of UniBern. Dr. Urs Eggenberger, Dr. Christoph Wanner, Christine Lemp and Dr. Andreas Jenni are especially thanked for always supporting me during my solid phase analysis.

Dr. Andreas Queisser from the Prüf- and Forschungsinstitut Sursee is thanked for his kind help with TG measurements. Silvia Köchli from PSI is thanked for the ICP-OES analysis.

Dr. Belay Dilnesa from EMPA/PSI is thanked for sharing his experience on AFm phases with me and for performing SEM measurements of my samples.

Dr. Peter Mandaliev from ETHZ is thanked for offering part of his beamtime, for me to measure some samples at the SLS-MS.

The beamline scientists of ESRF-DUBBLE (especially Sergey Nikitenko), ESRF-SNBL (especially Hermann Emerich and Wouter van Beek), and SLS-MS (especially Fabia Gozzo) are greatly acknowledged for their technical support.

The LDH group from Clermont-Ferrand is acknowledged for supporting my one-month stay there in 2009 by making room for my experiments. Dr. Fabrice Leroux is thanked for fruitful discussion during that time.

### ***LES members are greatly thanked for making my stay at PSI enjoyable:***

I would like to start by thanking Mike, for his welcome at LES from day one, and for his revision work on my publications. Beatrice is greatly thanked for her efficient help with office purposes.

Many thanks are addressed to the motivated technicians of LES accomplishing a remarkable work that I have hardly experienced in any other facilities before. I would like to thank you all, Werner, Vanessa, Andy, Astrid, Sabrina, and Dominik, for making my life in the lab so easy going. Special thanks go to Astrid for supervising my pyrite experiments and to Dominik for the cement-related ones, both answering my numerous phone calls and making themselves always available to kindly help me.

The tennis team (Wilfried, Bart, Dominik, Sergey, and Rainer) and the SOLA/running team (Georg, Thomas, Martin, Xavi, and Jan) deserve special thanks for giving a rhythm to my sportive year! Wine tasters and lovers (Bart, Marie, Nathalie, Jan, Erich, Rainer and Luc) are also warmly thanked for expovina sessions or for the introduction to the wine laboratory. The Euromillion team helped in every week giving me some adrenalin and hope for “plan A”: thank you Urs! Andreas is thanked for lending me many books that helped in increasing my curiosity level everyday. Tres is, to that respect, thanked for helping me find excuses for not always lending them all...!

My nice office mates from the present time and also from the past are greatly thanked for listening to my up and downs and for sharing laughs: Konstantin for sharing your knowledge on LDH phases and outdoor day breaks; Ferdinand for simultaneously sharing the good PhD steps as much as the more difficult ones; Luis for showing me that scientific passion does truly exist; Domy, Alyssa, and Fatima for giving me some insights on how it looks like to finish a PhD work!

I would like also to thank other LES young scientists who contributed to this nice environment. Xavi for your Catalan touch, Manav for your Indian flavors, and the women crew: Nathalie Diaz, Marie, Daniela, and Nathalie Macé for your friendships.

***Last but not least,***

***Many thanks to the people who encouraged me to start this PhD adventure:***

Based on my first nice summer at LES in 2005, I would like to thank Jan, Fatima, and Erich for strongly advising me to take this position. Special thanks go also to Jane Barling from UBC, who always supported me in believing that I could nicely achieve a PhD work and become a successful scientist.

These thanks are extended to my family, especially my parents and my godmother, and to my dear friends who have helped me to deal with the up and downs of what have eventually become: a success story.

## Table of Content

<b>Abstract.....</b>	<b>2</b>
<b>Chapter 1: Introduction.....</b>	<b>5</b>
1. Motivation of this study.....	6
1.1. Why is $^{129}\text{I}$ an issue for the management of radioactive waste?.....	6
1.2. Potential retention mechanisms for $^{129}\text{I}$ .....	7
1.3. Potential minerals for the retention of $^{129}\text{I}$ .....	9
1.4. Knowledge gap and objectives of present work.....	10
2. Properties of layered double hydroxides.....	11
2.1. Structural description.....	11
2.2. Industrial applications.....	14
2.3. Occurrence in the environment.....	14
2.4. Occurrence in nuclear waste.....	14
2.5. Occurrence in cement.....	15
3. Short introduction to the techniques.....	16
3.1. X-ray diffraction of powder materials.....	16
3.2. Extended X-ray absorption fine structure spectroscopy.....	19
3.3. Additional methods for the characterization of LDH.....	23
3.4. Thermodynamic modeling and database.....	25
4. Outline of the thesis.....	26
5. References.....	31
<b>Chapter 2: Iodide Interaction with Natural Pyrite.....</b>	<b>39</b>
<b>Chapter 3: Anion and Cation Order in Iodide-Bearing Mg/Zn-Al LDH.....</b>	<b>40</b>
<b>Chapter 4: Structural Insight into Iodide Uptake by AFm Phases.....</b>	<b>41</b>
<b>Chapter 5: Thermodynamics of AFm-(<math>\text{I}_2/\text{SO}_4</math>) Solid Solution in Aqueous Media.....</b>	<b>42</b>
<b>Chapter 6: Concluding Remarks and Future Work.....</b>	<b>43</b>
<b>Erklärung.....</b>	<b>47</b>
<b>Curriculum Vitae.....</b>	<b>48</b>

**Abstract**

The management of radioactive waste in Switzerland foresees the construction of a deep geological repository with a multi-barrier concept that includes a waste package (e.g. steel and cement materials), an engineered barrier (e.g. bentonite backfill and concrete) and a suitable geological host rock (e.g. the Opalinus Clay Formation) bearing a high sorption capacity and a low hydraulic permeability. Radioactive waste contains considerable amounts of the long-lived  $^{129}\text{I}$  radionuclide. Once released, iodide ( $\text{I}^-$ ) is the thermodynamically stable aqueous species for iodine under the anoxic repository conditions. The major solid phases in the host rock and in the engineered barriers foreseen for the deep geological repository (e.g. clay minerals) have negatively charged surfaces, and therefore they are unlikely to retard anions such as iodide. Due to its expected weak retention and long half-life,  $^{129}\text{I}$  is thus considered to be one of the dose-determining radionuclides released from an underground repository for radioactive waste.

This PhD work aimed at identifying and quantifying potential mechanisms for the retardation of  $^{129}\text{I}$  by sorption and/or incorporation processes onto and into minor minerals, which exist in the near- and far-field of a repository. Pyrite was first considered for the retention of  $^{129}\text{I}$ , because it is a minor mineral present in the Opalinus clay formation and in the bentonite buffer (up to 2 %), also because it has been reported to take up trace levels of iodide. In the frame of this study, experiments performed in a glove box ( $\text{O}_2 < 2$  ppm) using degassed Milli-Q water, i.e. under nearly-anoxic conditions, showed that iodide sorption by pyrite is too weak to contribute significantly to the retardation of  $^{129}\text{I}$  migration. Earlier studies performed in solid-solution equilibria open to air had likely suffered from oxidation.

In a second step, layered double hydroxides (LDH) were regarded as potential host phases for  $^{129}\text{I}$  owing to their occurrence in hydrated cement, a material locally abundant in the engineered barrier, and to their well-established ability to exchange anions. The structure of iodide-containing hydrotalcite-like LDH was first investigated at an atomic scale, revealing an ordered arrangement in the hydroxide layer of trivalent cations ( $\text{M}^{3+}$ ) with respect to the divalent ones ( $\text{M}^{2+}$ ) at  $\text{M}^{2+}$  over  $\text{M}^{3+}$  ratio of 3; only an ordered arrangement for a ratio of 2 had been reported until now. We have also demonstrated that cation ordering within LDH hydroxide layers has no effect on the location of iodide anions, displaying a local disorder similar to that of iodide anions in water.



Moreover, the uptake of trace levels of iodide by hydrated cement phases bearing positively-charged structural surfaces was quantified. Among ettringite, carbonate-containing Mg-Al LDH, chloride-, carbonate-, and sulfate-containing Ca-Al LDH (AFm phases), the sulfate-containing Ca-Al LDH (AFm-SO<sub>4</sub>) was found to be the only phase able to retain iodide. The reason for this preferential uptake was further investigated by a structural analysis of Ca-Al LDH, which contains two anions: iodide and a competitor anion (chloride, carbonate or iodide). A segregation of mono-iodide (AFm-I<sub>2</sub>) and Friedel's salt (AFm-Cl<sub>2</sub>) was found for coprecipitated I-Cl mixtures, whereas interstratifications of AFm-I<sub>2</sub> and hemicarboaluminate (AFm-OH-(CO<sub>3</sub>)<sub>0.5</sub>) were observed for the coprecipitated I-CO<sub>3</sub> system. Carbonate and chloride anions are thus expected to be strong competitors for the formation of iodide-containing AFm-I<sub>2</sub>. In contrast, a solid solution between AFm-I<sub>2</sub> and AFm-SO<sub>4</sub> for coprecipitated I-SO<sub>4</sub> mixtures was observed, and a short-range mixing of iodide and sulfate anions was found, allowing trace amounts of iodide to be immobilized by this cement hydration phase.

Finally, for improving long-term prediction of the fate of <sup>129</sup>I in the cementitious near field of a radioactive waste repository, a thermodynamic model was developed to describe the solid solution between AFm-SO<sub>4</sub> and AFm-I<sub>2</sub>. For this purpose, thermodynamic properties of AFm-I<sub>2</sub> and of its solid solution with AFm-SO<sub>4</sub> were evaluated based on precipitation and dissolution experiments. A satisfactory model was obtained by assuming a sub-regular solid solution behavior and by considering Vanselow's convention for the definition of the heterovalent mixing of sulfate and iodide end-members.

This PhD work highlighted the benefit of LDH phases, especially AFm-SO<sub>4</sub>, to incorporate iodide via the formation of solid solution. Up to now, thermodynamic models of hydrated ordinary Portland cement (OPC) suggest that AFm-SO<sub>4</sub> is not stable in a carbonate-containing system. However, this does not exclude the potential formation of solid solutions between AFm-SO<sub>4</sub> and AFm phases containing other anions that are not yet included in the thermodynamic database. Further investigations on the stability of solid solutions of AFm phases with multiple end-members including sulfate and other anions present in cementitious systems are therefore strongly recommended, as they could possibly show the stability of sulfate-containing solid solutions in thermodynamic predictions of OPC. Such data would help in understanding batch experiments where a considerable uptake of iodide onto carbonate-containing hydrated OPC has been measured.

Other AFm phases such as AFm-(OH)<sub>2</sub> and AFm-OH-(CO<sub>3</sub>)<sub>0.5</sub> were beyond the scope of this PhD work, but are also encouraged to be considered as potential phases for the uptake of <sup>129</sup>I. Other cement formulations than OPC such as calcium sulfoaluminate cement, in which AFm-SO<sub>4</sub> is thermodynamically stable, are currently not considered as engineered barrier materials. Such formulations require additional attention owing to their promising retention of anionic species. This work also encourages further study and interest in the possible uptake of other critical anionic radionuclides, e.g. <sup>99</sup>Tc (as TcO<sub>4</sub><sup>-</sup>) by LDH phases.

**Keywords:** <sup>129</sup>I, radioactive waste, iodine, pyrite, layered double hydroxides, hydrotalcite, AFm phases, wet chemistry, <sup>125</sup>I radiotracer experiments, EXAFS, XRD, thermodynamic modeling

## **Chapter 1: Introduction**

## 1. Motivation of this study

### 1.1. Why is $^{129}\text{I}$ an issue for the management of radioactive waste?

In Switzerland, it is planned to dispose of radioactive waste in two types of repository: one for spent fuel, vitrified high-level waste and long-lived intermediate level waste, and the other one for short-lived intermediate and low-level waste. The wastes arise from the operation of nuclear power plants, decommissioning, as well as medicine, industry and research (NAGRA, 2002). Both repositories are foreseen to be built underground in an adequate geological formation with a low hydraulic permeability. For instance, the Opalinus Clay has been identified to be an appropriate host rock for the high-level and long-lived intermediate-level waste repository type (NAGRA, 2002).

The function of an underground repository is to provide multiple barriers ensuring a slow migration of radionuclides, so that radioactive decay during radionuclides transport reduces the activity and residual doses in the biosphere to levels that never exceed the limits set by the regulators (NAGRA, 2002). In addition to the natural barrier, the repository system will include an engineered barrier to retard radionuclides mobility in the repository near-field. In the spent fuel and high-level waste repository, the engineered barrier will consist of steel canisters encapsulating the waste and of compacted bentonite (with a very low permeability) used to seal the repository tunnels. Intermediate- and low-level waste are solidified in concrete matrices and further surrounded by cementitious mortar and concrete.

Iodine-129 will be present in significant amounts in intermediate- and low-level waste and in spent fuel as it is one of the major long-lived fission products of nuclear chain reactions. Like other mobile fission products (e.g.,  $^{36}\text{Cl}$ ,  $^{14}\text{C}$ , and  $^{135}\text{Cs}$ )  $^{129}\text{I}$  is located preferentially in the gaps between the  $\text{UO}_2$  pellets and the cladding and at grain boundaries in high-level waste and will therefore be released soon after canister failure in the so-called “Instant Release Fraction” (JOHNSON et al., 2012). In both types of repository,  $^{129}\text{I}$  is expected to be released in the non-volatile iodide ( $\text{I}^-$ ) form to groundwater (NAGRA, 2002).

Under the neutral to alkaline pH conditions prevailing in a deep geological repository, major minerals of the host rock and the engineered barriers carry permanent negatively charged surfaces (e.g., interlayers of clay minerals in the Opalinus Clay or in the bentonite backfill). Radionuclides with a cationic speciation are thus retarded efficiently via surface complexation or ion exchange processes in clays (e.g., BRADBURY and BAEYENS, 2011). In contrast, anionic radionuclides like  $^{129}\text{I}$  are poorly

retained by such major minerals. Because  $^{129}\text{I}$  is very long-lived (half-life  $t_{1/2} = 15,700,000$  a), its radioactivity is not significantly reduced during its transport towards the biosphere, and this radionuclide is thus calculated to be a major contributor to the total radiological dose in safety assessment calculations (NAGRA, 2002). Therefore,  $^{129}\text{I}$  is one of the most problematic radionuclides.

However, one should keep in mind that a number of simplifying assumptions are made even in sophisticated safety assessment codes. For instance, chemical processes that could lead to decreased doses, but that are not sufficiently understood from a scientific point of view, are usually neglected in safety assessments for the sake of “conservatism”. A thorough understanding and quantification of processes able to bind iodine in their structure are necessary but are largely missing for implementation in safety calculations in view of reducing the dose contribution of  $^{129}\text{I}$ .

## 1.2. Potential retention mechanisms for $^{129}\text{I}$

“Sorption” is the generic term used in geochemistry for the uptake of trace levels of a given species by solid phases. Conceivable mechanisms for the sorption of radionuclides allowing their immobilization include surface adsorption, surface precipitation, precipitation, and coprecipitation. A brief summary of these processes is described below.

Surface adsorption for the retention of radionuclides or any other trace solute is considered to occur at mineral surfaces. The term mineral surfaces can relate to “external” surfaces directly exposed to the aqueous solution (e.g., “edge” surfaces in clay minerals), or to easily accessible surfaces in the inner parts of the mineral structure (e.g., the silicate interlayers in clay minerals). When adsorption occurs on external surfaces, it is thermodynamically considered as a surface complexation mechanism, limited by the available surface area and the density of sites accessible for the adsorption. Two major categories of surface complexes are commonly distinguished (e.g., STUMM and MORGAN, 1996): inner-sphere complexes, e.g., with a ligand exchange between the surface hydroxyl and  $\text{I}^-$  (eq. 1), or outer-sphere complexes, e.g., where  $\text{I}^-$  is attracted to the surface without loss of the hydration shell via electrostatic forces (eq. 2) like at the surface of hydrous ferric oxides (NAGATA et al., 2009).



where M is a metal ion and  $\equiv\text{M-OH}$  and  $\equiv\text{M-OH}_2^+$  are the protonated surface groups of metal (hydr)oxide compounds. Such complexation processes are largely dependent on the charge of the mineral surface and of the sorbing species (STUMM and MORGAN, 1996). Because of protonation/deprotonation reactions, the surface charge of most minerals is highly pH-dependent. The surface charge will be positive at pH below the point of zero charge  $\text{pH}_{\text{pzc}}$ , i.e., pH value at which the net electric charge of the surface is zero, and negative above this point. Hence, surface complexation of anions like  $\Gamma^-$  is usually insignificant above the  $\text{pH}_{\text{pzc}}$  and considerable below the  $\text{pH}_{\text{pzc}}$ , whereas cations will behave in the opposite way.

In contrast, when adsorption occurs at surfaces inherent to the structure, it occurs usually as ion exchange process, where the exchanged trace element replaces charge-compensating exchangeable ions from the structure. This process can also be considered as surface complexation. For example, an exchanged cation in clay minerals may be regarded as inner-sphere complex if the cation is directly coordinated to the silicate layer, or as outer-sphere complexation if the exchangeable cation is separated from the silicate layer by water molecules. From a thermodynamic point of view, such ion exchange processes can also be considered as formation of solid solutions involving the incorporation of two or more species into sites of a mineral lattice with a similar coordination environment. A beneficial effect of solid solution formation is that the solubility of a trace element forming a solid solution is lower than the solubility of the trace element when controlled by the pure solid alone. A true solid solution implies mixing (random or ordered) of the different species at an atomic scale. This can occur by the partial substitution of major ions occupying specific crystallographic sites by the trace element, e.g., the incorporation of iodide in a bromide-containing compound, where iodide occupies similar coordination sites as bromide, like the incorporation of iodide in silver bromide compounds (CHESSIN and VONNEGUT, 1971) (eq. 3).



Surface precipitation occurs at a pre-existing mineral surface and is a combination of surface complexation and precipitation. The sorbing element is first complexed at the mineral external surface. In a second step, it precipitates forming an epitaxial growth. If the mixing between substrate and surface precipitate is favored, i.e., by a low enthalpy of mixing, they may, from a thermodynamic point of view, subsequently form

a solid solution, or they may remain as separate phases (substrate and host mineral), if the mixing is not favored, i.e., with a large enthalpy of mixing.

Coprecipitation occurs when a soluble element simultaneously precipitates with another component. This term is non-specific and includes mechanical entrapment of a trace element as separate phase (e.g., into mixed crystals or occlusion) as well as its incorporation into the mineral structure (e.g., during mineral recrystallization). Thermodynamically, mechanical entrapment is considered as a mechanical mixing of two separate phases, one of them containing the trace element. The immobilization of a solute element in the case of mixed crystals is limited by the solubility of the resulting mixed phase, and in case of occlusion by the solubility of each independent phase. In contrast, the incorporation of a trace element into the mineral structure by coprecipitation can be thermodynamically considered as a solid solution formation, like in the case of ion exchange processes (eq. 4).

Finally, radionuclides may also precipitate as pure phases when dissolved species are present in sufficient concentration in solution to allow the supersaturation of a solid phase, i.e., when each constituent of the solid is present in greater amount than its solubility in the liquid. For example, sufficient quantities of  $\text{Ag}^+$  and  $\text{I}^-$  in solution, like the formation of AgI nanoparticles in presence of silver-containing mordenite (CHAPMAN et al., 2010), i.e., beyond the solubility limits of AgI, can allow the reaction described in eq. 1.4 to be displaced to the right. It is thermodynamically considered as a single phase.



Note that direct precipitation may be an important immobilization process for sparingly soluble cationic radionuclides, such as U and Pu, under the reducing conditions expected in a repository environment, but is not expected to play any role in the case of soluble anionic radionuclides such as  $^{129}\text{I}$ . Further explanations and examples of sorption mechanisms are given elsewhere (STUMM and MORGAN, 1996).

### 1.3. Potential minerals for the retention of $^{129}\text{I}$

Considering the potential retention mechanisms described above, minerals carrying positively charged surfaces under the chemical conditions in a repository (e.g., hydroxides, or minerals bearing hydroxide layers) are supposedly good candidates for surface adsorption of  $^{129}\text{I}$  as ( $\text{I}^-$ ).

Pyrite is present as a minor mineral in the host rock formation considered for the Swiss repository. Although pyrite does not carry positively charged surface at near-neutral pH, some authors claim the retention of trace levels of iodide by pyrite (FUHRMANN et al., 1998; STRICKERT et al., 1980). Besides, from a structural point of view, the ability of pyrite to incorporate iodide into its structure does not seem favored.

Hydrous ferric oxides (HFO) are among the common minerals bearing a positive surface charge under near-neutral conditions, and would thus be readily available for surface complexation (KAPLAN, 2003; NAGATA et al., 2009). Such HFO could therefore be considered for the retardation of  $^{129}\text{I}$  but were not investigated within the frame of this PhD work.

Another family of minerals to be considered for the retention of anionic species like  $\text{I}^-$  are the layered double hydroxide (LDH) and are also called “anionic clays” (KHAN and O'HARE, 2002; MIYATA, 1983) due to their positively charged hydroxide layers and their capacity to exchange anions from their interlayer space (Fig. 1), as clay minerals exchange cations from their interlayers.

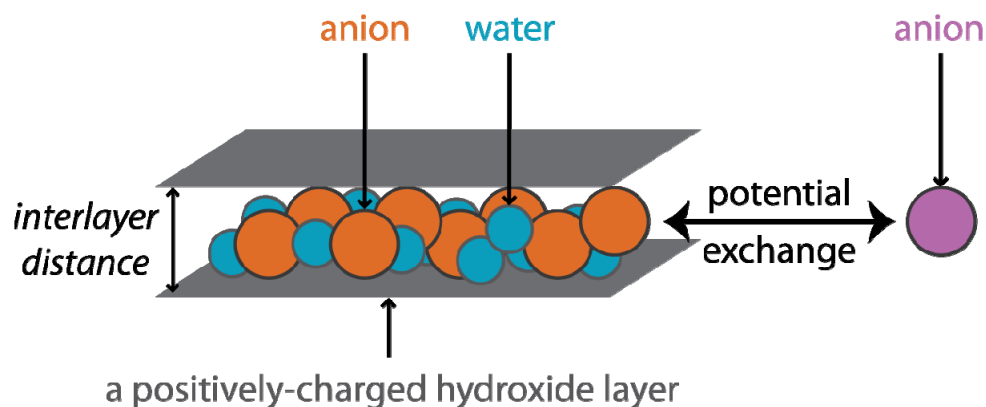


**Figure 1.** Layered double hydroxides: anionic exchangers

#### 1.4. Knowledge gap and objectives of present work

The objective of this PhD work was to evaluate the iodide binding mechanisms by selected minor minerals known to occur in the repository or in the host rock under the conditions expected in the planned Swiss repository system. Moreover, thermodynamic data that could be used to model the chemical fate of  $^{129}\text{I}$  were determined through careful experimental studies. Such knowledge may be used to improve predictions on the release of  $^{129}\text{I}$  into the biosphere and might ultimately reduce calculated doses in the safety analyses.



Pyrite was considered in a first approach of this Thesis work. Thanks to nearly anoxic conditions achievable nowadays and to a special care devoted to avoid oxidation phenomenon, an experimental study was conducted aiming at verifying the capacity of pyrite to retain iodide (see Chapter 2).

In a second approach, LDH phases have been investigated. The ability of LDH phases to exchange anions has generated strong interests in the past decades, in view of their potential for the retention of anionic contaminants. A relatively low affinity for iodide (e.g., compared to carbonate or chloride) was usually found in hydrotalcite-like LDH (BONTCHEV et al., 2003; CURTIUS and KATTILPARAMPIL, 2005; FETTER et al., 1999; KANG et al., 1999; KENTJONO et al., 2010; MIYATA, 1983; OLGUIN et al., 1998; PAREDES et al., 2006; PLESS et al., 2007). However, the current knowledge does not exclude the possible uptake of iodide in hydrocalumite-like LDH. A mechanistic understanding of the iodide incorporation into hydrotalcite-like and hydrocalumite-like LDH at an atomic level is still missing. In order to fill in this gap, a comprehensive structural study has been carried out during this PhD work (see Chapters 3 and 4).

Although a few thermodynamic data on LDH systems are available (ALLADA et al., 2002) including a recently obtained complete dataset for Mg(Fe-Al) hydrotalcite solid solution (ROZOV et al., 2011), data relevant for the uptake of anionic radionuclides via anionic exchange in LDH are still scarce (ALLADA et al., 2005; BALONIS et al., 2010; ISRAELI et al., 2000). In the present PhD study, the key thermodynamic properties characterizing the solid solution between the iodide and sulfate end-members of a Ca-Al LDH (the most favorable solid able to immobilize  $^{129}\text{I}$ ) were experimentally derived for the first time and successfully modeled (see Chapter 5). Such thermodynamic data are essential for safety analyses of a nuclear waste repository.

## 2. Properties of Layered Double Hydroxides

### 2.1. Structural description

LDH are composed of brucite-like layers (Fig. 2a) with a partial substitution of divalent by trivalent cations ( $\text{M}^{2+}$  by  $\text{M}^{3+}$ ) creating a net positive charge balanced by anions ( $\text{A}^{n-}$ ) intercalated in the interlayer space together with water molecules. The generic formula of LDH is  $\text{M}^{2+}_{1-r}\text{M}^{3+}_r(\text{OH})_2(\text{A}^{n-})_{r/n} \cdot i\text{H}_2\text{O}$  (DRITS and BOOKIN, 2001; EVANS and SLADE, 2006).

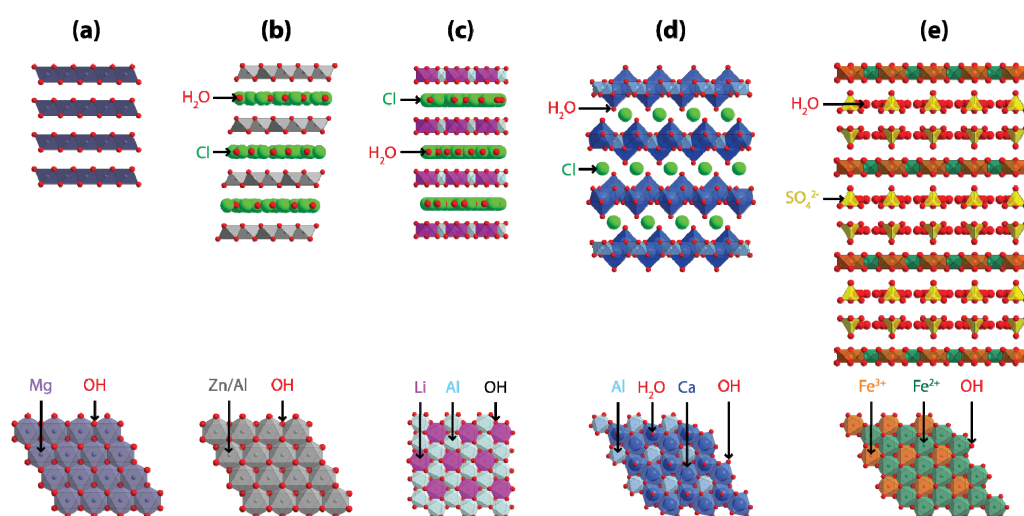


**Figure 2.** Structures of (a)  $\text{Mg}(\text{OH})_2$  (brucite); (b) ZnAl-Cl LDH LOMBARDO et al., 2005; (c) LiAl-Cl LDH BESSERGUENEV et al., 1997; (d) CaAl-Cl LDH (AFm-Cl<sub>2</sub>) RENAUDIN et al., 1999; (e)  $\text{Fe}^{2+}\text{Fe}^{3+}\text{-SO}_4$  LDH (green rust) SIMON et al., 2003.

LDH phases containing a ternary (e.g., DILNESA et al., 2011; ROZOV et al., 2010) or even a quaternary mixture (MARCHI and APESTEGUIA, 1998) of divalent and/or trivalent cations are reported to be stable by forming solid solution between two to four end-members. LDHs with  $\text{M}^{2+}$  and  $\text{M}^{3+}$  bearing similar ionic radii give rise to the hydroxalcite-like mineral family (e.g., with  $\text{Mg}^{2+}$  and  $\text{Al}^{3+}$ , Fig. 2b). LDHs with  $\text{M}^{2+}$  bearing ionic radii significantly larger than the one of the  $\text{M}^{3+}$  are part of the hydrocalumite mineral family (e.g., with  $\text{Ca}^{2+}$  and  $\text{Al}^{3+}$ , Fig. 2d). LDH with a monovalent cation have also been reported for lithium  $\text{LiAl}_2(\text{OH})_6(\text{A}^n)_{1/n} \cdot i\text{H}_2\text{O}$  (BESSERGUENEV et al., 1997) (Fig. 2c).

Interlayer anions and water molecules guarantee the bonding between successive hydroxide layers via a combination of electrostatic effects and hydrogen bonds. Both inorganic and organic anions can be intercalated in LDH (e.g., EVANS and SLADE, 2006). The size of the anion (when larger than the size of water molecules) usually determines the interlayer distance, which can extend up to  $\sim 20\text{-}22$  Å for large anions like DNA (DESIGAUX et al., 2006) or porphyrin (KAFUNKOVA et al., 2010) molecules. Anions usually form a single layer half way between two successive hydroxide layers (Fig. 2b, c, and d), but sometimes form two separate layers like in the case of green rust, a sulfate-containing  $\text{Fe}^{2+}\text{-Fe}^{3+}$  LDH (e.g., SIMON et al., 2003) (Fig. 2e). Such arrangements depend on the charge density per surface area unit for the interlayer species with respect to that of the hydroxide layers. Most LDH phases are constituted

by only one anionic species. However, LDH structures with interlayers alternating with two separate types of anions (so-called staging effect) have also been reported, especially in the case of organic-inorganic mixtures (TAVIOT-GUÉHO et al., 2010; TAVIOT-GUÉHO et al., 2005). The formation of a solid solution with different anionic species as end-members has also been described especially in the case of Ca-Al LDH (MESBAH et al., 2011) or with miscibility gaps for Mg-Al LDH (LEBAIL et al., 1987). Both staging and formation of a solid solution are described in this Thesis for iodide-containing Ca-Al LDH (Chapter 4).

LDHs usually crystallize in two types of stacking sequences (polytypes), with either a two-layer hexagonal stacking sequence (2H), or a three-layer rhombohedral sequence (3R), or also as an intergrowth of both polytypes with a relative proportion of 3R and 2H (THOMAS et al., 2004). Some LDH structures have also been reported as a one-layer sequence (1H) or as a six-layer rhombohedral or hexagonal sequence (6R or 6H) (DRITS and BOOKIN, 2001). Each type of sequence can display a variety of polytypes, depending on the ordering of the sequences, which have been further classified by Drits and Bookin (2H<sub>1</sub>, 2H<sub>2</sub>, 3R<sub>1</sub>...). The most common ones are the 3R<sub>1</sub> and 2H<sub>1</sub> polytypes, in which the interlayer sites (i.e., cavities between the hydroxide groups of adjacent layers) are prismatic (DRITS and BOOKIN, 2001; EVANS and SLADE, 2006).

Stacking faults and turbostratic distortion have also been widely reported for LDH systems and linked to a mismatch of chemistry/geometry between hydroxide layers and interlayer anions, preventing an ideal stacking (EVANS and SLADE, 2006). The (dis)order of cation and anion species at short- and long-range distances has a direct influence on the layer stacking and strongly depends on the LDH-type and on the anionic species. This is exemplified by the occurrence of phase transition for halide-containing Ca-Al LDH, where a rearrangement of interlayer species and a sliding of the stacking sequence takes place when the temperature is reduced, resulting in a lower symmetry (from a 3R into a 2H polytype for the chloride- and bromide-containing phases) (RENAUDIN et al., 2004). These structural details are still a matter of debates due to the usually low crystallinity of LDH phases. In recent reviews on LDH structures and characterization methods (DRITS and BOOKIN, 2001; EVANS and SLADE, 2006), emphasis is put on the usefulness of multi-tool approaches combining for example spectroscopic, thermodynamic, and molecular modeling investigations, allowing a better understanding of the arrangement and interplay between the hydroxide layer and the interlayer anions. Such a multi-tool approach has been applied in this PhD work (see Chapter 3).

## **2.2. Industrial applications**

With their low cost and ease of production the number of applications of LDHs has kept increasing in the past decade, especially for the hydrotalcite-like minerals. For example, LDHs have a large anion exchange capacity making them of large interest for entrapping organic and inorganic anions (e.g., pesticides, surfactants, nitrate, chromate), notably for the treatment of environmental and industrial waste waters. LDHs have also been considered as a successful support material for catalysts (organic synthesis, environmental catalysis, and natural gas conversion), as a host phase for photochemical reactions, or as a carrier for drug delivery. A review of all industrial applications has been given elsewhere (LI and DUAN, 2006).

## **2.3. Occurrence in the environment**

Hydrotalcite minerals can form under ambient conditions but are usually rare in nature (FORANO et al., 2006). Hydrotalcite minerals have been found for example in soils at the surface of phyllosilicates and gibbsite crystallites (e.g., SCHEIDEGGER et al., 1997). A Ni-Fe hydrotalcite was also found to be a product from the weathering of meteorites (CHUKANOV et al., 2009), and a Mg-Al hydrotalcite in sedimentary rocks of a rich Mg-Al clay (HALL and STAMATAKIS, 2000). Green rust was found in reductomorphic soils (TROLARD et al., 1997) and Ca-Al hydrocalumite in argillaceous marls (PASSAGLIA and SACERDOTI, 1988). Hydrotalcite-like minerals have also been reported to be present in industrial areas as a by-product from smelters or mining activities (CHAO and GAULT, 1997; JUILLOT et al., 2003; WITZKE, 1999; WITZKE and RAADE, 2000), where they can entrap contaminants. For example, the formation of sulfate-containing hydrotalcite in contaminated sites has been reported to help in immobilizing arsenic and chromate (ARDAU et al., 2011; DOUGLAS et al., 2010).

## **2.4. Occurrence in nuclear waste**

Mg-Al containing hydrotalcite-like minerals have been found to be one of the possible corrosion products of reactor fuel cladding in a saturated brine (MAZEINA et al., 2003), with a potential to act as an anionic exchanger for the other anionic radionuclides in nuclear waste. Mg-Al hydrotalcite is also expected to form as an alteration product of nuclear waste glass in presence of a salt brine, as reported for analogues of the reaction of seawater or MgCl<sub>2</sub> / CaCl<sub>2</sub> salts with a basaltic glass (ABDELOUAS et al., 1994; CROVISIER et al., 1986). Hydrotalcite-like minerals, especially, Mg-Fe-Al containing phases, are also expected to extensively form at the

clay cement interface of a nuclear waste repository (FERNANDEZ et al., 2010) and by interaction of corrosion products like nickel with cement (SCHEIDEGGER et al., 2006; VESPA et al., 2006).

## 2.5. Occurrence in cement

Portland cement is the most widely used cement type due to its large chemical and mechanical resistance and the low cost of reactants. Portland cement is presently foreseen for the construction of nuclear waste underground facilities and as a matrix for the immobilization of some radioactive waste forms (e.g., GLASSER, 2011). Portland cement contains typically 62-68% CaO, 21-24% SiO<sub>2</sub>, 5-14% Al<sub>2</sub>O<sub>3</sub>/Fe<sub>2</sub>O<sub>3</sub>, 0.5-4.5% MgO, and 1-3% SO<sub>3</sub> (e.g., GLASSER, 2011). Clinker material is produced by heating a mixture of mainly limestone with SiO<sub>2</sub> and Al<sub>2</sub>O<sub>3</sub> rich-materials (e.g., clay material) at elevated temperature (~1400°C). The cohesion of cement occurs during hydration of finely grinded clinker. Nowadays, for ordinary Portland cement (OPC), the clinker is also mixed with small amounts of gypsum and calcite (CaCO<sub>3</sub>).

The main hydration products of OPC include portlandite (Ca(OH)<sub>2</sub>), calcium silicate hydrate (C-S-H), calcite, ettringite (Ca<sub>6</sub>Al<sub>2</sub>(SO<sub>4</sub>)<sub>3</sub>(OH)<sub>12</sub>·26H<sub>2</sub>O), hydrotalcite (a carbonate- or hydroxide-containing Mg-Al LDH), and AFm phases (sulfate-, hydroxide-, chloride-, or carbonate-containing Ca-Al LDH) (GLASSER, 2011; LOTHENBACH and WINNEFELD, 2006). In OPC, the carbonate concentration has a strong influence on the phase assemblage (LOTHENBACH and WIELAND, 2006), e.g., in presence of carbonate, AFm-CO<sub>3</sub> is the expected AFm phase at equilibrium while sulfate will be mostly present in ettringite (LOTHENBACH and WINNEFELD, 2006).

Thermodynamic calculations predicting the full hydration of OPC (LOTHENBACH and WINNEFELD, 2006) show that C-S-H, portlandite, ettringite, and AFm-CO<sub>3</sub> only (i.e., absence of any other AFm phases) are the stable phases in presence of small amounts of carbonate (in equilibrium with calcite CaCO<sub>3</sub>). These results are in good agreement with experimental results (KUZEL, 1996), although the detection of small amounts of other AFm phases would be hardly detectable in such a complex chemical system. The authors of this hydration model for OPC (LOTHENBACH and WINNEFELD, 2006) stated that the given predictions are only a rough estimation, since they may not account for all solid solutions possibly present in the system. Therefore, the presence of AFm phases in OPC bearing other anions than carbonate, e.g., AFm-Cl<sub>2</sub> forming a solid solution with the AFm-CO<sub>3</sub> phase (MESBAH et al., 2011), cannot be ruled out.

From a structural point of view, the formation of a solid solution in AFm systems involving the main anionic species present in cementitious system has been reported elsewhere (e.g., MATSCHEI et al., 2007a; MESBAH et al., 2011) and requires special attention. Interest has also been paid to improve the thermodynamic evaluation of solid solutions in cementitious systems, for example, for AFm phases (e.g., BALONIS et al., 2010; DILNESA et al., 2011; LEISINGER et al., 2012; MATSCHEI et al., 2007a), AFt phases (e.g., LEISINGER et al., 2010), hydrogarnet (e.g., MATSCHEI et al., 2007b), hydrotalcite (e.g., ROZOV et al., 2010; ROZOV et al., 2011), and C-S-H (e.g., KULIK, 2011; WALKER et al., 2007). A complete understanding of the hydration products still requires additional thermodynamic data describing the formation of solid solutions in cementitious materials, notably the ones involving radionuclide species.

Hydration products strongly depend on the initial chemical composition of the clinker and reactant mixtures. A strong interest for modified OPC, e.g., the use of supplementary cementitious materials such as fly ash, slag, silica fume, and natural pozzolans added to clinker material has recently been given for improving the workability, durability and strength of the hardened cement paste (e.g., SHI et al., 2011).

A special care has also been devoted to evaluate the properties of calcium sulfoaluminate cements (CSA) for reducing the CO<sub>2</sub> production and lowering the firing temperature in the context of global warming (SHI et al., 2011). The clinker of CSA cement is produced by heating at ~1200°C a mixture of limestone, calcium sulfate and bauxite (a sedimentary rock containing a mixture of aluminium and iron oxide). Stable phases present after full hydration of CSA include ye'elimite, belite, anhydrite, Al(OH)<sub>3</sub>, strätlingite, ettringite, and AFm-SO<sub>4</sub> (WINNEFELD and LOTHENBACH, 2010). In contrast to OPC, calcite is not expected to be present in CSA, allowing AFm-SO<sub>4</sub> to be stable all along the hydration process, and, as it will be shown in this PhD work, maintaining a potential for uptake of anionic radionuclides.

### **3. Short introduction to the techniques**

#### **3.1. X-ray diffraction of powder materials**

X-ray powder diffraction (XRD) allows crystalline phases and their proportion in heterogeneous samples to be identified. In the case of pure phases, the crystallographic structure (cell parameters, atomic positions and strains) can be determined. However,

the structural resolution can be complex depending on the crystallinity and microstrains present in the material (e.g., small crystallite size and stacking faults in the case of LDH phases), which can result in modifications of position, intensity, width and shape of the diffracted peaks.

Measurements in reflection mode (Bragg-Brentano geometry) are the most common and conventional laboratory XRD equipment is usually sufficient to obtain satisfactory data. Measurements in transmission are favored for materials with preferential orientation, although they may require longer acquisition times, or the larger photon flux provided by synchrotron light, especially for low crystalline samples containing highly absorbing atoms.

In an ordered crystal, the direct (physical) space represents the periodic repetition of atom positions in the crystal and can be defined by the set of  $n$  points fulfilling the relationship:

$$n = u\vec{a} + v\vec{b} + w\vec{c} \quad (5)$$

where  $\vec{a}$ ,  $\vec{b}$ , and  $\vec{c}$  are linearly independent vectors, and  $u$ ,  $v$ , and  $w$  are integers.

$(\vec{a}, \vec{b}, \vec{c})$  forms the *Bravais* lattice of a crystal with

$(\vec{b}, \vec{c}) = \alpha$ ,  $(\vec{a}, \vec{c}) = \beta$ , and  $(\vec{a}, \vec{b}) = \gamma$  (see example in Fig. 3)

The reciprocal lattice is usually considered to define the orientation of a family of periodic planes, where the periodic repetition can also be represented by a set of vectors with:

$$\vec{a}^* = \frac{\vec{b} \times \vec{c}}{V}; \vec{b}^* = \frac{\vec{a} \times \vec{c}}{V}; \vec{c}^* = \frac{\vec{a} \times \vec{b}}{V} \quad (6)$$

$$\vec{S}^* = h\vec{a}^* + k\vec{b}^* + l\vec{c}^* \quad (7)$$

where  $V$  is the volume of the lattice  $(\vec{a}, \vec{b}, \vec{c})$  and  $h$ ,  $k$ , and  $l$  are integers known as Miller indices. The inverse of the norm of the diffraction vector  $\vec{S}^*$  corresponds to the distance between two consecutive planes of a family of  $hkl$  planes:  $d_{hkl}$ .

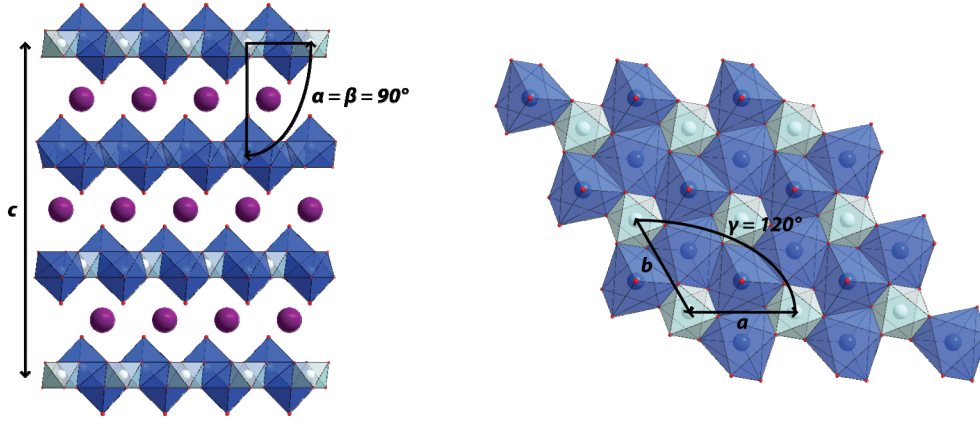


**Figure 3.** Structure of an iodide-containing Ca-Al LDH (AFm-I<sub>2</sub>) in R-3 space group. The cell parameters  $a$ ,  $b$ ,  $c$ ,  $\alpha$ ,  $\beta$  and  $\gamma$  are displayed.

When X-rays impinge on a regular array of scatterers (atoms in a crystalline sample), a regular array of spherical waves is produced, which are mostly cancelled out except in a few directions given by the Bragg law:

$$2d_{hkl} \cdot \sin(\theta) = n\lambda \quad (8)$$

where  $d_{hkl}$  is the interplanar spacing,  $\theta$  is the incident angle of the X-ray beam,  $n$  is the order of the reflection (any integer, usually 1),  $\lambda$  is the beam wavelength, where the measured reflections correspond to constructive interferences of the diffracted wave forming a  $2\theta$  angle with the incident beam. The amplitude of diffracted peaks can be calculated according to the following expressions:

$$A(hkl) = F(hkl) \cdot L(hkl) \quad (9)$$

$$F(hkl) = \sum_{j \text{ atoms}} f_j(\theta) \cdot e^{2\pi i(hx_j + hy_j + lz_j)} \quad (10)$$

$$L(hkl) = \sum_u \sum_v \sum_w e^{2\pi i(ha^*u + kb^*v + lc^*w)} \cdot (ua + vb + wc) \quad (11)$$

where  $A(hkl)$  is the amplitude of an  $hkl$  reflection,  $F(hkl)$  is the structure factor corresponding to the  $hkl$  reflection,  $f_j(\theta)$  is the individual atomic scattering factor tabulated in the international tables of the international union of crystallography, and  $L(hkl)$  is the form factor, which relates to the form and the size of the crystal.



Phase identification can be performed by a simple fingerprinting technique using a complete database such as the powder diffraction file (PDF). Cell parameters determination can be achieved by a profile fitting of a diffractogram (Le bail method) in a given space group owing to an accurate measurement of peaks positions over a large  $2\theta$  range. Furthermore, the entire crystal structure can be extracted by refining the powder diffraction data (Rietveld refinement), i.e., by fitting a calculated model to experimental intensities. The selected model takes into account the assumed crystal structure, the atomic positions, the instrumental factors obtained from refining a reference sample (usually a well-crystalline cubic mineral), and the strains. The refining tool from the Fullprof software was used in Chapter 3 (RODRIGUEZ-CARVAJAL, 1993; RODRIGUEZ-CARVAJAL, 2001). Despite their low crystallinity, a considerable amount of information related to the structure (location and bonding of the interlayer anion, stacking sequence) and to the microstructure of LDH can be obtained by XRD analysis of LDH powders. Further details about these methods are summarized elsewhere (EVANS and SLADE, 2006).

### **3.2. Extended X-ray absorption fine structure spectroscopy**

Extended X-ray absorption fine structure (EXAFS) spectroscopy allows the local environment around a targeted atom (the absorber atom) to be probed. Elements surrounding the absorber atom can be detected up to the third or even fourth coordination shell (up to  $\sim 6 \text{ \AA}$ ), but the EXAFS signal and the backscattering power of elements decrease by increasing the distance, and increase by increasing the atomic number of backscattering atoms. To get a satisfactory EXAFS signal for extracting structural information, not only an energetic and tunable X-ray beam is required, but also a high photon flux which is only accessible under synchrotron light. Transmission measurements require a sufficient amount of the X-ray absorber (e.g.,  $\sim 2\%$  for Zn and  $\sim 15\%$  for iodine). For dilute samples, the EXAFS signal can be instead collected in fluorescence or Auger mode. These techniques are also based on the absorption of X-rays with the emission of a core electron, but more specifically to the filling of core holes by electrons from higher energy shells, resulting in the release of X-ray (fluorescence) and in the emission of Auger electrons. All measurements presented in this PhD work were performed in transmission mode.

The absorption of X-rays is based on Beer-Lambert's law: when X-rays impinge on a sample, the transmitted intensity  $I$  can be defined as:

$$I = I_0 e^{-\mu x} \quad (12)$$

where  $I_0$  is the incident intensity,  $\mu$  is the absorption coefficient at a given energy, and  $x$  is the thickness of the sample crossed by the X-rays. The absorption function ( $\mu x$ ) measured by X-ray absorption spectroscopy (XAS) gradually decreases as a function of the energy, but once the energy reaches the binding energy of a core electron from atoms present in the sample (threshold energy  $E_0$ ), X-ray absorption greatly increases and the photon energy is sufficient to eject photo electrons from the core shells of the absorbing atom. The XAS technique is therefore element-specific, resulting in several absorption edges at specific  $E_0$  values. For instance,  $E_0$  at the K-edge of iodine, i.e., the energy required to eject a core electron from the K shell (the closest to the nucleus), is at 33169 eV when iodine is in its zero oxidation state (e.g.,  $I_2(s)$ ). The heavier the absorber atom is, the higher  $E_0$  is. For example, the K-edge of Zn ( $Z = 30$ ) is therefore below the one of iodine ( $Z = 53$ ), at 9659 eV when zinc is in its zero oxidation state (e.g., Zn metal). An X-ray absorption spectrum can be divided into three regions:

- (i) pre-edge region: some elements (e.g., Fe and Cr at the K-edge) exhibit a pre-edge feature which is due to interatomic transitions into free bound states below the Fermi energy. Such feature can be used to extract information on the oxidation state and in some cases on the coordination environment.
- (ii) X-ray absorption near-edge spectroscopy (XANES): energy range around the absorption edge at  $E_0$ . This region provides information on the absorber atom structure, notably its electronic configuration. For example, the position of the edge can give an indication of the oxidation state of the targeted element in the sample. The energy width of the absorption edge is a function of the mean free path, which represents the probability for the photoelectron to travel to the backscattering atom and to return without scattering or without the core hole to be filled in.
- (iii) EXAFS: region with oscillations of the absorption coefficient. EXAFS spectroscopy scans the energy after the edge of the absorber atom. The interaction between the photoelectron wave emanating from the absorber atom and the backscattered ones from neighboring atoms generates oscillations over a few hundreds eV after the edge in ordered condensed phases, typically solids. By modeling the EXAFS spectra, the nature of neighboring atoms (especially the distinction between light and heavy backscattering atoms), the distance and

coordination number between the absorber and backscattering atoms as well as the degree of order and of thermal motion (Debye-Waller factor) can be estimated.

The interference between the absorber atom and the backscattering atoms is linked to differences of the absorption coefficient according to eq. 13, and is usually represented as a function of the wave vector  $k$  ( $\text{\AA}^{-1}$ ). Note that the wave vector is directly linked to the energy scale (eq. 14).

$$\chi(k) = \frac{\mu(k) - \mu_0(k)}{\mu_0(k)} \quad (13)$$

$$k^2 = \frac{2m_{e^-}}{\hbar^2}(E - E_0) \quad (14)$$

where  $\mu(E)$  is the measured absorption,  $\mu_0(E)$  is the absorption of the isolated absorber atom (i.e., without neighbors),  $E$  is the energy of the incident photon,  $E_0$  is the threshold energy of the absorption process,  $m_{e^-}$  is the mass of an electron, and  $\hbar$  is the Planck constant. The EXAFS signal  $\chi_i(k)$  can be modeled with the single-scattering plane-wave EXAFS equation, which can be described at the K-edge according to eq. 15 (STERN and HEALD, 1983):

$$\chi_i(k) = \frac{N_i S_0^2 F_i(k)}{k R_i^2} \sin(2kR_i + \varphi_i(k)) e^{-2\sigma_i^2 k^2} e^{\frac{-2R_i}{\lambda(k)}} \quad (15)$$

where  $N_i$  is the degeneracy of path,  $S_0^2$  is the passive electron reduction factor,  $F_i(k)$  is the magnitude of the backscattering amplitude of the  $i^{\text{th}}$  neighbor atoms,  $k$  is the photoelectron wave vector,  $R_i$  is the mean distance between the absorber and the  $i^{\text{th}}$  shell,  $\varphi_i(k)$  is the phase shift due to the atomic potentials,  $\sigma_i$  is the relative mean square disorder parameter between the absorber and the atoms in the  $i^{\text{th}}$  shell, and  $\lambda(k)$  is the mean free path of the photoelectron caused by the finite core hole lifetime. The core hole lifetime is a function of  $k$ , i.e., the larger the energy is, the larger is the core-hole lifetime, and the broader is the absorption edge, e.g., for the I K-edge the full width at half maximum energy is of 10.6 eV, and of 1.67 eV for the Zn K-edge (KRAUSE and OLIVER, 1979).

Fourier Transform (FT) of  $\chi(k)$  yields a spectrum in real space, with peaks corresponding to individual coordination shells. The real part of the FT gives a radial

structure function (i.e., population of neighboring atoms around the absorber as a function of distance). Experimental EXAFS data from this work were fitted to ab initio models computed from 3D atomic models using the FEFF code (REHR et al., 1991) and the fitting tools available in the IFEFFIT software package (RAVEL and NEWVILLE, 2005) to determine the coordination environment around the absorber atom. Further explanations about the EXAFS technique are well detailed elsewhere (KONINGSBERGER and PRINS, 1987).

Iodine EXAFS spectroscopy at the L-edges has been mostly applied to the XANES region (e.g., FUHRMANN et al., 1998; REED et al., 2002; SCHLEGEL et al., 2006; YAMAGUCHI et al., 2006), because of the short energy ranges between  $L_I$  and  $L_{II}$  edges (336 eV) and between  $L_{II}$  and  $L_{III}$  edges (295 eV), corresponding to short  $k$ -ranges 9.3 and  $8.7 \text{ \AA}^{-1}$ , respectively. Such short  $k$ -ranges have been used for example in studies about iodide ions in aqueous solution (FULTON et al., 2010), i.e., with structural information limited to the hydration shell. In contrast, larger  $k$ -ranges are accessible at the K-edge, although the oscillations are relatively weak and the energy width of the absorption edge is relatively large (BONHOURE et al., 2002). In earlier studies iodine K-edge XAS has been mostly limited to the near edge range (XANES) due to the weak oscillations at room temperature (BONHOURE et al., 2002; KODAMA et al., 2006; REED et al., 2002; SHIMAMOTO and TAKAHASHI, 2008; YAMAGUCHI et al., 2006). Only a few EXAFS studies were performed at the I K-edge, either at room temperature for physical studies on atomic iodine (GOMILSEK et al., 2009), iodide ions in water (FULTON et al., 2010; TANIDA and WATANABE, 2000),  $KIO_3$  (YAGI et al., 2001), ZnSe:I compounds (LEZAMA-PACHECO et al., 2004), and tetramethylammonium (D'ANGELO et al., 2008), or below 20 K to solve more complex matrices including iodine-doped carbon nanotubes (MICHEL et al., 2006) and aromatic vs. aliphatic organoiodide compounds (FEITERS et al., 2005).

The EXAFS measurements presented in this Thesis were performed at the K-edge and the samples were cooled at 15 K using a He cryostat to limit thermal motion, and therefore greatly improving both  $k$ -space resolution and amplitude of the oscillations. EXAFS measurements were carried out using a pair of Si(111) crystals at the DUBBLE beamline of the European synchrotron radiation facility (ESRF, Grenoble, France). The Darwin width of the Si(111) crystals at the I K-edge is considerably large (8.6 eV, vs e.g., 1.8 eV for the Si(311) crystal). For this reason, a special care was given to the selection of the energy calibration of the absorption edge during data analysis.

The EXAFS technique has been previously used to understand the structure of LDH phases at an atomic scale. For instance, the demonstration of special EXAFS features of cationic species in LDH compared to other compounds like hydroxides or phyllosilicates (SCHEINOST et al., 1999; SCHEINOST and SPARKS, 2000) allowed the speciation analysis of complex matrices (e.g., soils, cement) (DEGRYSE et al., 2011; JACQUAT et al., 2008; ROBERTS et al., 1999; ROBERTS et al., 2003; SCHEIDEGGER et al., 2006; VESPA et al., 2006; VOEGELIN et al., 2011; VOEGELIN and KRETZSCHMAR, 2005). EXAFS spectroscopy was also used for purely structural analysis, for example to determine the short-range cation order (FUNKE et al., 2007; FUNKE et al., 2005; INTISSAR et al., 2003; ROUSSEL et al., 2001; TAVIOT-GUEHO et al., 2005). It has also been successfully applied for determining the coordination environment of complex anionic species, notably for Mo and Cr-containing LDH (MALHERBE et al., 1999; VAYSSE et al., 2002), showing that the geometry of these anions in LDH is very similar to the one in their salts, and to get more insight into the intercalation processes (BEAUDOT et al., 2004; LIU et al., 2006). A complete review of the use of the EXAFS technique for LDH systems has been reported elsewhere (EVANS and SLADE, 2006).

Most recent uses are also summarized in Chapter 3, where EXAFS spectroscopy has been applied for investigating both short-range cation order in the hydroxide layer (at the Zn K-edge) and single anion (at the I K-edge) order in the interlayer. In Chapter 4, EXAFS spectroscopy at the I K-edge was used for studying the coordination environment of iodide in Ca-Al LDH in presence of other anions.

### 3.3. Additional methods for the characterization of LDH

Porosity, surface area, and morphology/particle size are important criteria for the potential industrial applications of LDHs and are often studied by means of N<sub>2</sub> adsorption/desorption isotherm measurements applying the Brunauer Emmet Teller (BET) model, and scanning/transmission electron microscope (SEM or TEM), respectively. LDHs with surface areas ranging from 100 to 300 m<sup>2</sup> are excellent candidates for catalysis purposes (LI and DUAN, 2006). The porosity can be well-controlled by the intercalation of organic polymers allowing for instance properties of supercapacitors to be enhanced (STIMPFLING and LEROUX, 2010; TAVIOT-GUÉHO and LEROUX, 2006). LDH phases grow as small (< 1 μm) platelets and usually aggregate in a sand rose-like morphology (Fig. 4a, KHENIFI et al., 2009). After long equilibration time, LDHs may also homogeneously grow to form large hexagonal micro-sized

platelets, like the AFm-I<sub>2</sub> platelets prepared in this PhD work, which were formed after 84 days of equilibration (see sample description in Chapter 4) (Fig. 1.4b).

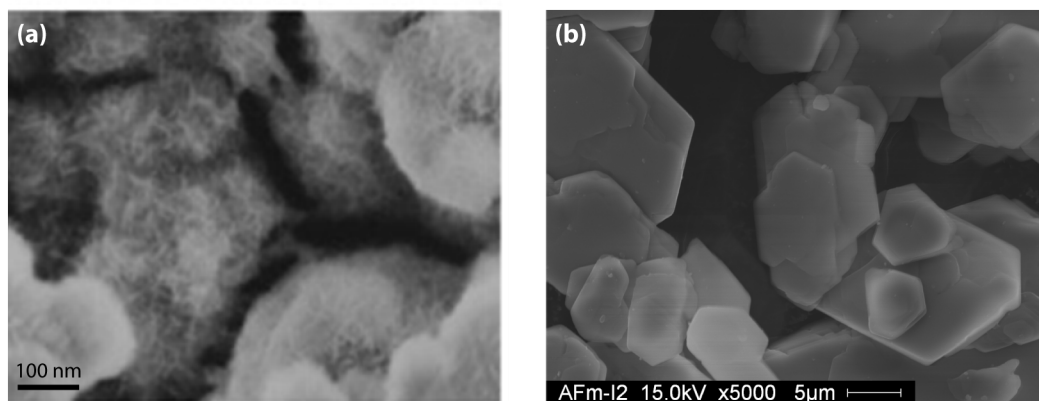


**Figure 4.** SEM image of synthetic (a) sand-roses morphology of Ni-Al LDH thin films KHENIFI et al., 2009 and (b) large hexagonal AFm-I<sub>2</sub> platelets, SEM image by courtesy of Dr. Belay Dilnesa (Empa).

A complete understanding of LDH properties requires also the intercalation process to be kinetically and mechanistically identified at an atomic scale. Using time-resolved energy dispersive XRD techniques such processes have been shown to occur within minutes (WILLIAMS et al., 2006), and the formation of staging intermediates could be better apprehended (TAVIOT-GUÉHO et al., 2010). The intercalation mechanism is also closely related to the dynamic and orientation of anions in the interlayer, which requires an atomic-scale resolution of such structures. Apart from XRD and EXAFS spectroscopy, nuclear magnetic resonance (NMR), infrared (IR) and Raman spectroscopy techniques have been applied to provide some insight into the orientation of interlayer species, which is highly specific to the molecular geometry of the intercalated anions (EVANS and SLADE, 2006). For example, carbonate ions in Ca-Al LDH are oriented parallel to the layer structure, while nitrate-containing Ca-Al LDH display a pillared layered structure with nitrate ions bridging two adjacent hydroxide layers (RENAUDIN et al., 2000). In addition, molecular dynamic (MD) simulations have been developed specifically for LDH systems allowing a better understanding of the dynamic of interlayer species (CYGAN et al., 2009; KALINICHEV and KIRKPATRICK, 2002).

### 3.4. Thermodynamic modeling and database

Geochemical models that facilitate long-term predictions of the behavior of radionuclides in a nuclear waste repository need to be developed. For this purpose, speciation calculations are required to describe thermodynamic equilibria between aqueous species and solid phases occurring (or expected) in this environment. Such calculations are usually performed using chemical codes based on the law of mass action (e.g., PHREEQC code, PARKHURST and APPELO, 1999) or the Gibbs energy minimization (e.g., GEM-Selektor code, KULIK et al., 2004). Whereas the law of mass action codes calculate overall equilibrium by satisfying all the reaction constants required to be at equilibrium, the total Gibbs free energy of a system is minimized at a given temperature and pressure in the GEMS code. This method is particularly efficient and straightforward for chemical systems that include solid solution phases and was used in the present work. Various activity models for aqueous species are available in GEMS and can be selected depending on the ionic strength of the given system. Here, we used an extended Debye-Hückel equation appropriate for the moderate ionic strength of the modeled solutions.

The reliability of the results obtained from such codes critically depends on a good knowledge of standard-state molar properties of the chemical species of interest and on reliable interaction parameters in between aqueous species. A thorough review of thermodynamic data for the major (solid, aqueous, and gaseous) species of the elements potentially present in the geological surroundings of a nuclear waste repository was carried out by the laboratory for waste management at PSI, leading to the compilation of the Nagra-PSI (v.01/01) database (HUMMEL et al., 2002). This database is implemented in GEMS and is used in the present study along with a database especially derived for the main components present in hydrated Portland cement (LOTHENBACH and WINNEFELD, 2006; MATSCHEI et al., 2007b). In addition, thermodynamic data for the main aqueous, solid, and gaseous iodine species were derived and implemented in GEMS for this PhD study from available published data, and will be implemented in the updated version of the Nagra-PSI database currently under development.

As mentioned in section 1.2., one of the possible mechanisms to retain radionuclides into the structure of major phases of the repository environment is the formation of solid solution with host phases bearing an affinity for the radionuclides. In order to assess the chemical equilibria between solid solutions and the aqueous phase, corresponding thermodynamic models have to usually be experimentally derived. A

time-consuming but precise method for assessing the thermodynamic stability of solid phases (including solid solutions) is solubility experiments, which were carried out in this work (see Chapter 5). Such experiments consisted of series of precipitation (supersaturation) and dissolution (undersaturation) experiments, after which the compositions of the solid and liquid phases at equilibrium were analyzed and combined to yield solubility products. Appropriate analytical methods were developed for the analysis of the solid and liquid phases and are explained in Chapter 5.

For pure phases, the computation of solid phases is straightforward, whereas the solubility product of solid solutions must be computed using the so-called Lippmann's functions. A thorough description of the method for developing such a model as well as the determination of the Gibbs free energy of a single solid phase is detailed in Chapter 5, taking the example of AFm-I<sub>2</sub> – AFm-SO<sub>4</sub> solid solution.

## 4. Outline of the Thesis

The PhD Thesis is composed of four studies aiming at understanding possible pathways of <sup>129</sup>I retardation and corresponding uptake mechanisms capable of binding iodide in a nuclear waste repository. Each chapter is a research article, and these articles are currently at different stages of the publication process. An introductory chapter (no. 1) and a concluding chapter (no. 6) provide the proper context and an overarching discussion and outlook. Below is a short account of each chapter, including the role and contributions of a substantial number of collaborators from various research laboratories, where parts of the Thesis work were performed.

**Chapter 2:** Iodide Interaction with Natural Pyrite (2011). **Laure Aimoz**, Enzo Curti, and Urs Mäder. *Journal of radionalytical and nuclear chemistry*. **288**(2). 517-524.

*I set up the experimental work under the supervision of Enzo Curti, performed the experiments and analyzed the obtained data. Support for the data analysis and especially the thermodynamic evaluation was provided by Enzo Curti. Urs Mäder and Enzo Curti participated in the data interpretation. I wrote the manuscript under the main supervision of Enzo Curti, which was further improved by Urs Mäder.*



Earlier studies claimed the potential of pyrite to take up trace levels of iodide (FUHRMANN et al., 1998; STRICKERT et al., 1980). However, no detailed uptake mechanisms were proposed. Because a negative surface-charge of pyrite is expected for experiments carried out at near-neutral pH, electrostatic binding of anions like iodide is not expected. These studies were performed in solid- aqueous solution equilibria open to air, and have likely suffered from oxidation.

The motivation of this paper was to perform similar experiments but under the nearly anoxic conditions achievable nowadays with advanced laboratory equipments, such as in nitrogen-filled glove boxes. A small but measureable uptake of iodide by pyrite was observed and attributed to the partial oxidation of the pyrite surface generating a positively-charged surface at near-neutral pH (FUHRMANN et al., 1998; STRICKERT et al., 1980). In spite of many efforts to avoid any oxygenation of the system, the amount of dissolved oxygen in equilibrium with the trace levels of gaseous oxygen in the atmosphere of the glove box was calculated to be sufficient to oxidize small regions of the pyrite surface. Therefore, the observed weak uptake of iodide is probably due to undesired oxidation effects. It could be concluded that pyrite will not contribute significantly to the retardation of  $^{129}\text{I}$  release from a nuclear waste repository and other materials, like the layered double hydroxides, were considered in a second stage of the PhD work resulting in the following chapters.

**Chapter 3:** Anion and Cation Order in Iodide-Bearing Mg/Zn-Al Layered Double Hydroxides (2012). **Laure Aimoz**, Christine Taviot-Guého, Sergey V. Churakov, Marina Chukalina, Rainer Dähn, Enzo Curti, Pierre Bordet, and Marika Vespa. *The Journal of Physical Chemistry C*. 116(9): 5460-5475.

*This work was the result of multiple collaborations, to make the structural analysis as thorough as possible owing to a broad interdisciplinary approach. This study was initiated by Enzo Curti. I performed the synthesis of the studied phase under the main supervision of Christine Taviot-Guého in her home institution (Laboratoire des Matériaux Inorganiques, Université Blaise Pascal, Clermont Ferrand, France). The EXAFS measurements were possible thanks to in-house synchrotron beamtime granted to Marika Vespa while she was working as a beamline scientist at the Dutch-Belgian beamline of the European synchrotron radiation facility (ESRF, Grenoble, France). The data were collected by myself, Enzo Curti, Rainer Dähn, and Marika Vespa. The*

*synchrotron XRD measurements were performed at the French national synchrotron facility (SOLEIL, Gif-sur-Yvette) during a beamtime allocated to Christine Taviot-Guého. Marika Vespa trained me for EXAFS data analysis, which was further supervised by Rainer Dähn. Marina Chukalina performed the FEFF-based wavelet calculations and helped me in the interpretation of the corresponding data. I performed the XRD data analysis with strong support by Christine Taviot-Guého for the Rietveld refinement. The pair distribution function analysis was done by Christine Taviot-Guého with the help of Pierre Bordet. Sergey Churakov performed all ab initio simulations and helped me in their integration for the paper discussion. I did the data interpretation with great help of Christine Taviot-Guého. Except the sections on ab initio calculations written by Sergey Churakov and on pair distribution function written by Christine Taviot-Guého, I wrote the manuscript under the supervision of Christine Taviot-Guého. The manuscript was further improved by all co-authors and by Urs Mäder.*

A molecular-level understanding of iodide-bearing LDH phases is essential for understanding their thermodynamic stability and, ultimately, their potential to retard the migration of  $^{129}\text{I}$  released from nuclear waste. The aim of this paper was to elucidate the atomic structure of iodide-containing (Mg/Zn-Al) LDH and to improve the still incomplete knowledge on the charge distribution and interlayer structure in LDH systems.

Complementary methods allowed a fine structure analysis of such LDH at different atomic scales to be determined. First, EXAFS spectroscopy at the Zn and I K-edges was used as a local probe (up to 8 Å) of both cations and interlayer anions coordination environments. In addition to conventional multi-shell fitting a recent development to analyze EXAFS spectra, the FEFF-based wavelet transform method, was applied. This method provides a precise localization and identification of cations within LDH hydroxide layers. Short and medium-range information (up to 50 Å) could be obtained with the analysis of the pair distribution function (PDF) of synchrotron X-ray powder diffraction data. The good quality of the synchrotron X-ray powder diffraction data also enabled us to perform a Rietveld refinement of the structure and to obtain valuable microstructural information (size of coherent domains, level of microstrains). Finally, our experimental findings and interpretations were supported by geometry optimization of the structures using ab initio calculations. The combination of these advanced techniques allowed us to show for the first time a locally-ordered distribution of cations in LDHs for a  $\text{M}^{2+}/\text{M}^{3+}$  molar ratio of 3. We also could demonstrate

unambiguously that an ordered distribution of trivalent and divalent cations in the hydroxide layer has no influence on the distribution of anions in the interlayer.

**Chapter 4:** Structural Insight into Iodide Uptake by AFm Phases. **Laure Aimoz**, Erich Wieland, Christine Taviot-Guého, Rainer Dähn, Marika Vespa, and Sergey Churakov. *Environmental Science & Technology*. DOI: 10.1021/es204470e.

*I prepared the experimental design of this paper under the supervision of Erich Wieland, and I performed all laboratory work and XRD measurements. I collected the low temperature XRD measurements during the allocated beamtime at the Swiss Norwegian beamline of the ESRF, with the help of Enzo Curti. EXAFS data were collected by myself, Marika Vespa, and Rainer Dähn, during the allocated synchrotron beamtime at the Dutch-Belgian beamline of the ESRF. I carried out the XRD measurements and analyzed the data under the supervision of Christine Taviot-Guého. I performed EXAFS data analysis under the supervision of Rainer Dähn. Sergey Churakov performed all ab initio simulations and helped me in their integration for the paper discussion. I interpreted all the data, with the inputs and advice from Sergey Churakov and Erich Wieland. Except the section on ab initio calculations written by Sergey Churakov, I wrote the manuscript under the supervision of Erich Wieland. Further improvements of the manuscript were made by all co-authors, by Enzo Curti, and by Urs Mäder.*

The aim of this study was to improve our molecular-level understanding of the processes controlling the immobilization of iodide in the cementitious materials based on previous studies showing the uptake of trace levels of iodide by bulk cement (BONHOURE et al., 2002; POINTEAU et al., 2008). In this study, evidence was found that the LDH AFm-SO<sub>4</sub> is the phase responsible for the retention of iodide in the cement matrix. The reasons for the preferential uptake of iodide by AFm-SO<sub>4</sub> among other cementitious AFm phases were investigated by means of bi-anionic synthesis and characterization of the solid using XRD and EXAFS spectroscopy. EXAFS at the I K-edge was applied here for the first time to iodide-containing cement minerals and allowed a molecular-level understanding on iodide binding in the interlayer of AFm phases. The study shows the formation of solid solution between monosulfate (AFm-SO<sub>4</sub>) and monoiodide (AFm-I<sub>2</sub>) at ambient temperature with short-range mixing of iodide and sulfate, while a segregation of mono-iodide (AFm-I<sub>2</sub>) and Friedel's salt

(AFm-Cl<sub>2</sub>) was found for coprecipitated I-Cl mixtures, and interstratifications of AFm-I<sub>2</sub> and hemicarboaluminate (AFm-OH-(CO<sub>3</sub>)<sub>0.5</sub>) were observed for coprecipitated I-CO<sub>3</sub> system.

The capability of AFm-SO<sub>4</sub> to act as a sink for the hazardous <sup>129</sup>I was demonstrated, which has potential consequences for the assessment of iodide immobilization in connection with the safe disposal of radioactive waste. The findings from this study further allowed conclusions to be drawn concerning the design of the cementitious encapsulation matrix and the effect of competing anions, such as chloride and carbonate, on the long-term safe disposal of iodide. The finding from this chapter initiated the study described in the following chapter.

**Chapter 5:** Thermodynamics of AFm-(I<sub>2</sub>, SO<sub>4</sub>) Solid Solution and of its End-Members in Aqueous Media. **Laure Aimoz**, Dmitrii A. Kulik, Erich Wieland, Enzo Curti, Barbara Lothenbach, and Urs Mäder. *Submitted for publication.*

*I prepared the experimental design of this paper under the supervision of Erich Wieland and Barbara Lothenbach. I performed all solubility experiments. Enzo Curti and to a large extent Dmitrii Kulik trained me in thermodynamic modeling techniques. Data interpretation was also supported by fruitful scientific advice of Urs Mäder and Barbara Lothenbach. I wrote the manuscript under the supervision of Erich Wieland, Enzo Curti, and Dmitrii Kulik. Further improvements of the manuscript were made by the other co-authors.*

For the performance assessment of a nuclear waste repository, reliable geochemical models are required to predict the fate of radionuclides. This study was motivated by the evidence of a solid solution formation between iodide and sulfate mixing in AFm phases and aimed at assessing the stability of the solid solution with AFm-SO<sub>4</sub>.

The thermodynamic properties of AFm-SO<sub>4</sub>, a hydration product of various cement formulations, were determined elsewhere and available from literature. In contrast, the properties of pure AFm-I<sub>2</sub> were not yet available. A large series of precipitation-dissolution and sorption experiments were carried out with the aim of assessing the thermodynamic properties of the AFm-I<sub>2</sub> end-member and modeling its solid solution with AFm-SO<sub>4</sub>. Special attention was devoted to the determination of the Gibbs free energy of this solid solution, which is not necessarily straightforward for heterovalent mixtures. The thermodynamic data presented in this paper are judged to have sufficient

quality for implementation into critically reviewed thermodynamic databases, and will therefore help predicting the fate of  $^{129}\text{I}$  in the cementitious near field of a nuclear waste repository.

## 5. References

- Abdelouas, A., Crovisier, J. L., Lutze, W., Fritz, B., Mosser, A., and Muller, R., 1994. Formation of Hydrotalcite-Like Compounds during R7t7 Nuclear Waste Glass and Basaltic Glass Alteration. *Clays Clay Miner.* **42**, 526-533.
- Allada, R. K., Navrotsky, A., Berbeco, H. T., and Casey, W. H., 2002. Thermochemistry and aqueous solubilities of hydrotalcite-like solids. *Science* **296**, 721-723.
- Allada, R. K., Pless, J. D., Nenoff, T. M., and Navrotsky, A., 2005. Thermochemistry of hydrotalcite-like phases intercalated with  $\text{CO}_3^{2-}$ ,  $\text{NO}_3^-$ ,  $\text{Cl}^-$ ,  $\text{I}^-$ , and  $\text{ReO}_4^-$ . *Chem. Mater.* **17**, 2455-2459.
- Ardau, C., Cannas, C., Fantauzzi, M., Rossi, A., and Fanfani, L., 2011. Arsenic removal from surface waters by hydrotalcite-like sulphate minerals: field evidences from an old mine in Sardinia, Italy. *Neues Jahrbuch für Mineralogie (Abhandlungen)* **188**, 49-63.
- Balonis, M., Lothenbach, B., Le Saout, G., and Glasser, F. P., 2010. Impact of chloride on the mineralogy of hydrated Portland cement systems. *Cem. Concr. Res.* **40**, 1009-1022.
- Besserguenev, A. V., Fogg, A. M., Francis, R. J., Price, S. J., OHare, D., Isupov, V. P., and Tolochko, B. P., 1997. Synthesis and structure of the gibbsite intercalation compounds  $[\text{LiAl}_2(\text{OH})_6]\text{X}$   $\{\text{X}=\text{Cl}, \text{Br}, \text{NO}_3\}$  and  $[\text{LiAl}_2(\text{OH})_6]\text{Cl}\cdot\text{H}_2\text{O}$  using synchrotron X-ray and neutron powder diffraction. *Chem. Mater.* **9**, 241-247.
- Bonhoure, I., Scheidegger, A. M., Wieland, E., and Dähn, R., 2002. Iodine species uptake by cement and CSH studied by I K-edge X-ray absorption spectroscopy. *Radiochim. Acta* **90**, 647-651.
- Bontchev, R. P., Liu, S., Krumhansl, J. L., Voigt, J., and Nenoff, T. M., 2003. Synthesis, characterization, and ion exchange properties of hydrotalcite  $\text{Mg}_6\text{Al}_2(\text{OH})_{16}\text{A}_x\text{A}'_{(2-x)}\cdot 4\text{H}_2\text{O}$  ( $\text{A}, \text{A}' = \text{Cl}^-, \text{Br}^-, \text{I}^-$ , and  $\text{NO}_3^-$ ,  $2 \geq x \geq 0$ ) derivatives. *Chem. Mater.* **15**, 3669-3675.
- Bradbury, M. H. and Baeyens, B., 2011. Predictive sorption modelling of Ni(II), Co(II), Eu(III), Th(IV) and U(VI) on MX-80 bentonite and Opalinus Clay: A "bottom-up" approach. *App. Clay Sci.* **52**, 27-33.
- Chao, G. Y. and Gault, R. A., 1997. Quintinite-2H, quintinite-3T, charmarite-2H, charmarite-3T and caresite-3T, a new group of carbonate minerals related to the hydrotalcite-manasseite group. *Can. Mineral.* **35**, 1541-1549.
- Chapman, K. W., Chupas, P. J., and Nenoff, T. M., 2010. Radioactive iodine capture in silver-containing mordenites through nanoscale silver iodide formation. *J. Am. Chem. Soc.* **132**, 8897-8899.
- Chessin, H. and Vonnegut, B., 1971. Lattice spacings of pseudobinary solid solutions of silver bromide and silver iodide. *J. Am. Chem. Soc.* **93**, 4964-4966.
- Chukanov, N. V., Pekov, I. V., Levitskaya, L. A., and Zadov, A. E., 2009. Droninoite,  $\text{Ni}_3\text{Fe}^{3+}\text{Cl}(\text{OH})_8\cdot 2\text{H}_2\text{O}$ , a New Hydrotalcite-Group Mineral Species from the Weathered Dronino Meteorite. *Geology of Ore Deposits* **51**, 767-773.

- Crovisier, J. L., Fritz, B., Grambow, B., and Eberhart, J. P., 1986. Dissolution of basaltic glass in seawater: experiments and thermodynamic modelling. In: Pittsburgh (Ed.) *Scientific basis for nuclear waste management IX*. Materials Research Society, Stockholm, Sweden.
- Curtius, H. and Kattilparampil, Z., 2005. Sorption of iodine on Mg-Al-layered double hydroxide. *Clay Miner.* **40**, 455-461.
- Cygan, R. T., Greathouse, J. A., Heinz, H., and Kalinichev, A. G., 2009. Molecular models and simulations of layered materials. *J. Mater. Chem.* **19**, 2470-2481.
- D'Angelo, P., Zitolo, A., Migliorati, V., and Pavel, N. V., 2008. Measurement of x-ray multielectron photoexcitations at the I K-edge. *Phys. Rev. B* **78**, 144105.
- Degryse, F., Voegelin, A., Jacquat, O., Kretzschmar, R., and Smolders, E., 2011. Characterization of zinc in contaminated soils: complementary insights from isotopic exchange, batch extractions and XAFS spectroscopy. *Eur. J. Soil Sci.* **62**, 318-330.
- Desigaux, L., Ben Belkacem, M., Richard, P., Cellier, J., Leone, P., Cario, L., Leroux, F., Taviot-Gueho, C., and Pitard, B., 2006. Self-assembly and characterization of layered double hydroxide/DNA hybrids. *Nano Lett.* **6**, 199-204.
- Dilnesa, B. Z., Lothenbach, B., Le Saout, G., Renaudin, G., Mesbah, A., Filinchuk, Y., Wichser, A., and Wieland, E., 2011. Iron in carbonate containing AFm phases. *Cem. Concr. Res.* **41**, 311-323.
- Douglas, G. B., Wendling, L. A., Pleysier, R., and Trefry, M. G., 2010. Hydrotalcite formation for contaminant removal from Ranger mine process water. *Mine Water Environ.* **29**, 108-115.
- Drits, V. A. and Bookin, A. S., 2001. Crystal structure and X-ray identification of layered double hydroxides. In: Rives, V. (Ed.), *Layered Double Hydroxides: Present and Future*. Nova Science Publishers inc., New York.
- Evans, D. G. and Slade, R. C. T., 2006. Structural aspects of layered double hydroxides. In: Duan, X., Evans, D.G. (Ed.), *Layered Double Hydroxides*. Springer-Verlag, Berlin Heidelberg 2005.
- Feiters, M. C., Kupper, F. C., and Meyer-Klaucke, W., 2005. X-ray absorption spectroscopic studies on model compounds for biological iodine and bromine. *J. Synchrotron Rad.* **12**, 85-93.
- Fernandez, R., Cuevas, J., and Mäder, U. K., 2010. Modeling experimental results of diffusion of alkaline solutions through a compacted bentonite barrier. *Cem. Concr. Res.* **40**, 1255-1264.
- Fetter, G., Olguin, M. T., Bosch, P., Lara, V. H., and Bulbulian, S., 1999. <sup>131</sup>I sorption from aqueous solutions by nitrated hydrotalcites. *J. Radioanal. Nucl. Chem.* **241**, 595-599.
- Forano, C., Hibino, T., Leroux, F., and Taviot-Guého, C., 2006. Layered Double Hydroxides. In: Bergaya, F., Theng, B.K.G., and Lagaly, G. (Ed.), *Handbook of Clay Science*. Elsevier Ltd., Amsterdam (The Netherlands).
- Fuhrmann, M., Bajt, S., and Schoonen, M. A. A., 1998. Sorption of iodine on minerals investigated by X-ray absorption near edge structure (XANES) and I-125 tracer sorption experiments. *Appl. Geochem.* **13**, 127-141.
- Fulton, J. L., Schenter, G. K., Baer, M. D., Mundy, C. J., Dang, L. X., and Balasubramanian, M., 2010. Probing the hydration structure of polarizable halides: a multiedge XAFS and molecular dynamics study of the iodide anion. *J. Phys. Chem. B* **114**, 12926-12937.
- Funke, H., Scheinost, A. C., and Chukalina, M., 2005. Wavelet analysis of extended x-ray absorption fine structure data. *Phys. Rev. B* **71**, 094110.
- Funke, H., Chukalina, M., and Scheinost, A. C., 2007. A new FEFF-based wavelet for EXAFS data analysis. *J. Synchrotron Rad.* **14**, 426-432.

- Glasser, F. P., 2011. Application of inorganic cements to the conditioning and immobilisation of radioactive wastes. In: Ojovan, M. I. (Ed.), *Handbook of advanced radioactive waste conditioning technologies*. Woodhead Publishing, Cambridge, UK.
- Gomilsek, J. P., Arcon, I., de Panfilis, S., and Kodre, A., 2009. X-ray absorption in atomic iodine in the K-edge region. *Phys. Rev. A* **79**, 032514.
- Hall, A. and Stamatakis, M. G., 2000. Hydrotalcite and an amorphous clay mineral in high-magnesium mudstones from the Kozani Basin, Greece. *J. Sediment. Res.* **70**, 549-558.
- Hummel, W., Berner, U., Curti, E., Pearson, F. J., and Thoenen, T., 2002. *Nagra/PSI thermodynamic database 01/01*. Universal Publisher/uPublish.com, Parkland, Florida.
- Intissar, M., Jumas, J. C., Besse, J. P., and Leroux, F., 2003. Reinvestigation of the layered double hydroxide containing tetravalent cations: Unambiguous response provided by XAS and Mossbauer spectroscopies. *Chem. Mater.* **15**, 4625-4632.
- Israeli, Y., Taviot-Guého, T., Beese, J. P., Morel, J. P., and Morel-Desrosiers, N., 2000. Thermodynamics of anion exchange on a chloride-intercalated zinc-aluminum layered double hydroxide: a microcalorimetric study. *J. Chem. Soc., Dalton Trans.*, 791-796.
- Jacquat, O., Voegelin, A., Villard, A., Marcus, M. A., and Kretzschmar, R., 2008. Formation of Zn-rich phyllosilicate, Zn-layered double hydroxide and hydrozincite in contaminated calcareous soils. *Geochim. Cosmochim. Acta* **72**, 5037-5054.
- Johnson, L., Günther-Leopold, I., Kobler Waldis, J., Linder, H. P., Low, J., Cui, D., Ekeröth, E., Spahiu, K., and Evins, L. S., 2012. Rapid aqueous release of fission products from high burn-up LWR fuel: Experimental results and correlations with fission gas release. *J. Nucl. Mater.* **420**, 54-62.
- Juillot, F., Morin, G., Ildefonse, P., Trainor, T. P., Benedetti, M., Galoisy, L., Calas, G., and Brown, G. E., 2003. Occurrence of Zn/Al hydrotalcite in smelter-impacted soils from northern France: Evidence from EXAFS spectroscopy and chemical extractions. *Am. Mineral.* **88**, 509-526.
- Kafunkova, E., Lang, K., Kubat, P., Klementova, M., Mosinger, J., Slouf, M., Troutier-Thuilliez, A. L., Leroux, F., Verney, V., and Taviot-Gueho, C., 2010. Porphyrin-layered double hydroxide/polymer composites as novel ecological photoactive surfaces. *J. Mater. Chem.* **20**, 9423-9432.
- Kalinichev, A. G. and Kirkpatrick, R. J., 2002. Molecular dynamics modeling of chloride binding to the surfaces of calcium hydroxide, hydrated calcium aluminate, and calcium silicate phases. *Chem. Mater.* **14**, 3539-3549.
- Kang, M. J., Chun, K. S., Rhee, S. W., and Do, Y., 1999. Comparison of sorption behavior of I<sup>-</sup> and TcO<sub>4</sub><sup>-</sup> on Mg/Al layered double hydroxide. *Radiochim. Acta* **85**, 57-63.
- Kaplan, D. I., 2003. Influence of surface charge of an Fe-oxide and an organic matter dominated soil on iodide and pertechnetate sorption. *Radiochim. Acta* **91**, 173-178.
- Kentjono, L., Liu, J. C., Chang, W. C., and Irawan, C., 2010. Removal of boron and iodine from optoelectronic wastewater using Mg-Al (NO<sub>3</sub>) layered double hydroxide. *Desalination* **262**, 280-283.
- Khan, A. I. and O'Hare, D., 2002. Intercalation chemistry of layered double hydroxides: recent developments and applications. *J. Mater. Chem.* **12**, 3191-3198.

- Khenifi, A., Derriche, Z., Forano, C., Prevot, V., Mousty, C., Scavetta, E., Ballarin, B., Guadagnini, L., and Tonelli, D., 2009. Glyphosate and glufosinate detection at electrogenerated NiAl-LDH thin films. *Anal. Chim. Acta* **654**, 97-102.
- Kodama, S., Takahashi, Y., Okumura, K., and Uruga, T., 2006. Speciation of iodine in solid environmental samples by iodine K-edge XANES: Application to soils and ferromanganese oxides. *Sci. Total Environ.* **363**, 275-284.
- Koningsberger, D. C. and Prins, R., 1987. *X-ray absorption: principles, applications, techniques of EXAFS, SEXAFS, and XANES*. John Wiley & Sons, New York.
- Krause, M. O. and Oliver, J. H., 1979. Natural widths of atomic K-levels and L-levels, K-alpha X-ray-lines and several Kll auger lines. *J. Phys. Chem. Ref. Data* **8**, 329-338.
- Kulik, D. A., Berner, U., and Curti, E., 2004. Modelling chemical equilibrium partitioning with the GEMS-PSI code. In: Smith, B. a. G., B. (Eds.) *PSI scientific Report 2003 / Volume IV, Nuclear Energy and Safety*. Paul Scherrer Institut, Villigen, Switzerland.
- Kulik, D. A., 2011. Improving the structural consistency of C-S-H solid solution thermodynamic models. *Cem. Concr. Res.* **41**, 477-495.
- Kuzel, H. J., 1996. Initial hydration reactions and mechanisms of delayed ettringite formation in Portland cements. *Cem. Concr. Compos.* **18**, 195-203.
- Lebail, C., Thomassin, J. H., and Touray, J. C., 1987. Hydrotalcite-like solid-solutions with variable  $\text{SO}_4^{2-}$  and  $\text{CO}_3^{2-}$  contents at 50 degrees C - an X-ray-diffraction and Raman-spectrometry study. *Phys. Chem. Miner.* **14**, 377-382.
- Leisinger, S. M., Lothenbach, B., Le Saout, G., Kagi, H., Wehrli, B., and Johnson, C. A., 2010. Solid solutions between  $\text{CrO}_4^-$  and  $\text{SO}_4^-$ -ettringite  $\text{Ca}_6(\text{Al}(\text{OH})_6)_2[(\text{CrO}_4)_x(\text{SO}_4)_{1-x}]_3 \cdot 26 \text{H}_2\text{O}$ . *Environ. Sci. Technol.* **44**, 8983-8988.
- Leisinger, S. M., Lothenbach, B., Le Saout, G., and Johnson, C. A., 2012. Thermodynamic modeling of solid solutions between monosulfate and monochromate  $3\text{CaO} \cdot \text{Al}_2\text{O}_3 \cdot \text{Ca}[(\text{CrO}_4)_x(\text{SO}_4)_{1-x}] \cdot n\text{H}_2\text{O}$ . *Cem. Concr. Res.* **42**, 158-165.
- Lezama-Pacheco, J., de Leon, J. M., Espinosa, F. J., Rabago, F., and Conradson, S., 2004. Local atomic structure around iodine in ZnSe:I. *Sol. Energy Mater. Sol. Cells* **82**, 151-157.
- Li, F. and Duan, X., 2006. Applications of Layered Double Hydroxides. In: Evans, D. G. and Slade, R. C. T. (Eds.) *Layered Double Hydroxides*. Springer-Verlag, Berlin Heidelberg.
- Lombardo, G. M., Pappalardo, G. C., Punzo, F., Costantino, F., Costantino, U., and Sisani, M., 2005. A novel integrated X-ray powder diffraction (XRPD) and molecular dynamics (MD) approach for modelling mixed-metal (Zn, Al) layered double hydroxides (LDHs). *Eur. J. Inorg. Chem.* **24**, 5026-5034.
- Lothenbach, B. and Wieland, E., 2006. A thermodynamic approach to the hydration of sulphate-resisting Portland cement. *Waste Manage.* **26**, 706-719.
- Lothenbach, B. and Winnefeld, F., 2006. Thermodynamic modelling of the hydration of Portland cement. *Cem. Concr. Res.* **36**, 209-226.
- Malherbe, F., Bigey, L., Forano, C., de Roy, A., and Besse, J. P., 1999. Structural aspects and thermal properties of takovite-like layered double hydroxides pillared with chromium oxo-anions. *J. Chem. Soc., Dalton Trans.*, 3831-3839.
- Marchi, A. J. and Apestequia, C. R., 1998. Impregnation-induced memory effect of thermally activated layered double hydroxides. *App. Clay Sci.* **13**, 35-48.
- Matschei, T., Lothenbach, B., and Glasser, F. P., 2007a. The AFm phase in Portland cement. *Cem. Concr. Res.* **37**, 118-130.



- Matschei, T., Lothenbach, B., and Glasser, F. P., 2007b. Thermodynamic properties of Portland cement hydrates in the system  $\text{CaO-Al}_2\text{O}_3\text{-SiO}_2\text{-CaSO}_4\text{-CaCO}_3\text{-H}_2\text{O}$ . *Cem. Concr. Res.* **37**, 1379-1410.
- Mazeina, L., Curtius, H., and Fachinger, J., 2003. Formation of hydrotalcite-like compounds during corrosion experiments on MTR-Fe-Al cladding. *Clay Miner.* **38**, 35-40.
- Mesbah, A., Cau-Dit-Coumes, C., Frizon, F., Leroux, F., Ravaux, J., and Renaudin, G., 2011. A new investigation of the  $\text{Cl}^- \text{-CO}_3^{2-}$  substitution in AFm phases. *J. Am. Ceram. Soc.* **94**, 1901-1910.
- Michel, T., Alvarez, L., Sauvajol, J. L., Almairac, R., Aznar, R., Bantignies, J. L., and Mathon, O., 2006. EXAFS investigations of iodine-doped carbon nanotubes. *Phys. Rev. B* **73**, 195419.
- Miyata, S., 1983. Anion-exchange properties of hydrotalcite-like compounds. *Clays Clay Miner.* **31**, 305-311.
- Nagata, T., Fukushi, K., and Takahashi, Y., 2009. Prediction of iodide adsorption on oxides by surface complexation modeling with spectroscopic confirmation. *J. Colloid Interface Sci.* **332**, 309-316.
- Nagra, 2002. Technical Report. NTB 02-05. Nagra, Wettingen, Switzerland.
- Olguin, M. T., Bosch, P., Acosta, D., and Bulbulian, S., 1998.  $^{131}\text{I}$  sorption by thermally treated hydrotalcites. *Clays Clay Miner.* **46**, 567-573.
- Paredes, S. P., Fetter, G., Bosch, P., and Bulbulian, S., 2006. Iodine sorption by microwave irradiated hydrotalcites. *J. Nucl. Mater.* **359**, 155-161.
- Parkhurst, D. L. and Appelo, C. A. J., 1999. User's guide to PHREEQC (Version 2) - A computer program for speciation, batch reaction, one-dimensional transport and inverse geochemical calculations. *U.S. Geological Survey water resources investigations report* U.S. Geological Survey, Denver, USA.
- Passaglia, E. and Sacerdoti, M., 1988. Hydrocalumite from Montalto Di Castro, Viterbo, Italy. *Neues Jahrbuch für Mineralogie-Monatshefte*, 454-461.
- Pless, J. D., Chwirka, J. B., and Krumhansl, J. L., 2007. Iodine sequestration using delafossites and layered hydroxides. *Environ. Chem. Lett.* **5**, 85-89.
- Pointeau, I., Coreau, N., and Reiller, P. E., 2008. Uptake of anionic radionuclides onto degraded cement pastes and competing effect of organic ligands. *Radiochim. Acta* **96**, 367-374.
- Ravel, B. and Newville, M., 2005. ATHENA, ARTEMIS, HEPHAESTUS: data analysis for X-ray absorption spectroscopy using IFEFFIT. *J. Synchrotron Rad.* **12**, 537-541.
- Reed, W. A., May, I., Livens, F. R., Charnock, J. M., Jeapes, A. P., Gresley, M., Mitchell, R. M., and Knight, P., 2002. XANES fingerprinting of iodine species in solution and speciation of iodine in spent solvent from nuclear fuel reprocessing. *J. Anal. At. Spectrom.* **17**, 541-543.
- Rehr, J. J., Deleon, J. M., Zabinsky, S. I., and Albers, R. C., 1991. Theoretical X-ray absorption fine-structure standards. *J. Am. Chem. Soc.* **113**, 5135-5140.
- Renaudin, G., Kubel, F., Rivera, J. P., and Francois, M., 1999. Structural phase transition and high temperature phase structure of Friedels salt,  $3\text{CaO}\cdot\text{Al}_2\text{O}_3\cdot\text{CaCl}_2\cdot 10\text{H}_2\text{O}$ . *Cem. Concr. Res.* **29**, 1937-1942.
- Renaudin, G., Rapin, J. P., Humbert, B., and Francois, M., 2000. Thermal behaviour of the nitrated AFm phase  $\text{Ca}_4\text{Al}_2(\text{OH})_{12}(\text{NO}_3)_2\cdot 4\text{H}_2\text{O}$  and structure determination of the intermediate hydrate  $\text{Ca}_4\text{Al}_2\text{OH}_{12}(\text{NO}_3)_2\cdot 2\text{H}_2\text{O}$ . *Cem. Concr. Res.* **30**, 307-314.
- Renaudin, G., Rapin, J. P., Elkaim, E., and Francois, M., 2004. Polytypes and polymorphs in the related Friedel's salt  $[\text{Ca}_2\text{Al}(\text{OH})_6]^+[\text{X}\cdot 2\text{H}_2\text{O}]^-$  halide series. *Cem. Concr. Res.* **34**, 1845-1852.

- Roberts, D. R., Scheidegger, A. M., and Sparks, D. L., 1999. Kinetics of mixed Ni-Al precipitate formation on a soil clay fraction. *Environ. Sci. Technol.* **33**, 3749-3754.
- Roberts, D. R., Ford, R. G., and Sparks, D. L., 2003. Kinetics and mechanisms of Zn complexation on metal oxides using EXAFS spectroscopy. *J. Colloid Interface Sci.* **263**, 364-376.
- Rodriguez-Carvajal, J., 1993. Recent advances in magnetic-structure determination by neutron powder diffraction. *Physica B* **192**, 55-69.
- Rodriguez-Carvajal, J., 2001. Recent developments of the program Fullprof, *Commission on Powder Diffraction (IUCr) Newsletter*.
- Roussel, H., Briois, V., Elkaim, E., de Roy, A., Besse, J. P., and Jolivet, J. P., 2001. Study of the formation of the layered double hydroxide [Zn-Cr-Cl]. *Chem. Mater.* **13**, 329-337.
- Rozov, K., Berner, U., Taviot-Gueho, C., Leroux, F., Renaudin, G., Kulik, D., and Diamond, L. W., 2010. Synthesis and characterization of the LDH hydrotalcite-pyroaurite solid-solution series. *Cem. Concr. Res.* **40**, 1248-1254.
- Rozov, K. B., Berner, U., Kulik, D. A., and Diamond, L. W., 2011. Solubility and Thermodynamic Properties of Carbonate-Bearing Hydrotalcite-Pyroaurite Solid Solutions with a 3:1 Mg/(Al+Fe) Mole Ratio. *Clays Clay Miner.* **59**, 215-232.
- Scheidegger, A. M., Lamb, G. M., and Sparks, D. L., 1997. Spectroscopic evidence for the formation of mixed-cation hydroxide phases upon metal sorption on clays and aluminum oxides. *J. Colloid Interface Sci.* **186**, 118-128.
- Scheidegger, A. M., Vespa, M., Grolimund, D., Wieland, E., Harfouche, M., Bonhoure, I., and Dahn, R., 2006. The use of (micro)-X-ray absorption spectroscopy in cement research. *Waste Manage.* **26**, 699-705.
- Scheinost, A. C., Ford, R. G., and Sparks, D. L., 1999. The role of Al in the formation of secondary Ni precipitates on pyrophyllite, gibbsite, talc, and amorphous silica: A DRS study. *Geochim. Cosmochim. Acta* **63**, 3193-3203.
- Scheinost, A. C. and Sparks, D. L., 2000. Formation of layered single- and double-metal hydroxide precipitates at the mineral/water interface: A multiple-scattering XAFS analysis. *J. Colloid Interface Sci.* **223**, 167-178.
- Schlegel, M. L., Reiller, P., Mercier-Bion, F., Barre, N., and Moulin, V., 2006. Molecular environment of iodine in naturally iodinated humic substances: Insight from X-ray absorption spectroscopy. *Geochim. Cosmochim. Acta* **70**, 5536-5551.
- Shi, C. J., Jimenez, A. F., and Palomo, A., 2011. New cements for the 21st century: The pursuit of an alternative to Portland cement. *Cem. Concr. Res.* **41**, 750-763.
- Shimamoto, Y. S. and Takahashi, Y., 2008. Superiority of K-edge XANES over L-III-edge XANES in the speciation of iodine in natural soils. *Anal. Sci.* **24**, 405-409.
- Simon, L., Francois, M., Refait, P., Renaudin, G., Lelaurain, M., and Genin, J. M. R., 2003. Structure of the Fe(II-III) layered double hydroxysulphate green rust two from Rietveld analysis. *Solid State Sci.* **5**, 327-334.
- Stern, E. A. and Heald, S. M., 1983. Basic principles and Applications of EXAFS. In: Koch, E. (Ed.), *Handbook of Synchrotron Radiation*. North-Holland, Amsterdam, New York.
- Stimpfling, T. and Leroux, F., 2010. Supercapacitor-type behavior of carbon composite and replica obtained from hybrid layered double hydroxide active container. *Chem. Mater.* **22**, 974-987.
- Strickert, R., Friedman, A. M., and Fried, S., 1980. The sorption of technetium and iodine radioisotopes by various minerals. *Nucl. Technol.* **49**, 253-266.

- Stumm, W. and Morgan, J. J., 1996. *Aquatic chemistry: chemical equilibria and rates in natural waters*. Wiley-Interscience Publications, New York.
- Tanida, H. and Watanabe, I., 2000. Dependence of EXAFS (extended X-ray absorption fine structure) parameters of iodide anions in various solvents upon a solvent parameter. *Bull. Chem. Soc. Jpn.* **73**, 2747-2752.
- Taviot-Guého, C., Leroux, F., Payen, C., and Besse, J. P., 2005. Cationic ordering and second-staging structures in copper-chromium and zinc-chromium layered double hydroxides. *App. Clay Sci.* **28**, 111-120.
- Taviot-Guého, C. and Leroux, F., 2006. In situ polymerization and intercalation of polymers in layered double hydroxides. In: Evans, D. G. and Slade, R. C. T. (Eds.) *Layered Double Hydroxides*. Springer-Verlag, Berlin Heidelberg.
- Taviot-Guého, C., Feng, Y. J., Faour, A., and Leroux, F., 2010. Intercalation chemistry in a LDH system: anion exchange process and staging phenomenon investigated by means of time-resolved, in situ X-ray diffraction. *Dalton T.* **39**, 5994-6005.
- Thomas, G. S., Rajamathi, M., and Kamath, P. V., 2004. DIFFaX simulations of polytypism and disorder in hydrotalcite. *Clays Clay Miner.* **52**, 693-699.
- Trolard, F., Genin, J. M. R., Abdelmoula, M., Bourrie, G., Humbert, B., and Herbillon, A., 1997. Identification of a green rust mineral in a reductomorphic soil by Mossbauer and Raman spectroscopies. *Geochim. Cosmochim. Acta* **61**, 1107-1111.
- Vaysse, C., Guerlou-Demourgues, L., Demourgues, A., Lazartigues, F., Fertier, D., and Delmas, C., 2002. New (Ni, Co)-based layered double hydroxides with intercalated oxometalate (Mo, W) species, obtained by chimie douce reactions. *J. Mater. Chem.* **12**, 1035-1043.
- Vespa, M., Dahn, R., Grolimund, D., Wieland, E., and Scheidegger, A. M., 2006. Spectroscopic investigation of Ni speciation in hardened cement paste. *Environ. Sci. Technol.* **40**, 2275-2282.
- Voegelin, A. and Kretzschmar, R., 2005. Formation and dissolution of single and mixed Zn and Ni precipitates in soil: Evidence from column experiments and extended X-ray absorption fine structure spectroscopy. *Environ. Sci. Technol.* **39**, 5311-5318.
- Voegelin, A., Jacquat, O., Pfister, S., Barmettler, K., Scheinost, A. C., and Kretzschmar, R., 2011. Time-dependent changes of zinc speciation in four soils contaminated with zincite or sphalerite. *Environ. Sci. Technol.* **45**, 255-261.
- Walker, C. S., Savage, D., Tyrer, M., and Ragnarsdottir, K. V., 2007. Non-ideal solid solution aqueous solution modeling of synthetic calcium silicate hydrate. *Cem. Concr. Res.* **37**, 502-511.
- Williams, G. R., Khan, A. I., and O'Hare, D., 2006. Mechanistic and kinetic studies of guest ion intercalation into layered double hydroxides using time-resolved, in-situ X-ray powder diffraction. In: Duan, X., Evans, D.G. (Ed.), *Layered Double Hydroxides*. Springer-Verlag, Berlin Heidelberg 2005.
- Winnefeld, F. and Lothenbach, B., 2010. Hydration of calcium sulfoaluminate cements - Experimental findings and thermodynamic modelling. *Cem. Concr. Res.* **40**, 1239-1247.
- Witzke, T., 1999. Hydrowoodwardite, a new mineral of the hydrotalcite group from Königswalde near Annaberg, Saxony/Germany and other localities. *Neues Jahrbuch für Mineralogie-Monatshefte*, 75-86.
- Witzke, T. and Raade, G., 2000. Zincowoodwardite,  $[Zn_{1-x}Al_x(OH)_2][(SO_4)_{x/2}(H_2O)_n]$ , a new mineral of the hydrotalcite group. *Neues Jahrbuch für Mineralogie-Monatshefte*, 455-465.

- Yagi, K., Umezawa, S., Terauchi, H., and Kasatani, H., 2001. EXAFS study of phase transitions in  $\text{KIO}_3$ . *J. Synchrotron Rad.* **8**, 803-805.
- Yamaguchi, N., Nakano, M., Tanida, H., Fujiwara, H., and Kihou, N., 2006. Redox reaction of iodine in paddy soil investigated by field observation and the I K-edge XANES fingerprinting method. *J. Environ. Radioact.* **86**, 212-226.

## Chapter 2: Iodide Interaction with Natural Pyrite

Reproduced with permission from "Iodide Interaction with Natural Pyrite (2011). **Laure Aimoz**, Enzo Curti, and Urs Mäder. *Journal of radionalytical and nuclear chemistry*. **288**(2). 517-524." Copyright 2012 Springer.

This article is available on <http://www.springerlink.com/>

### **Chapter 3: Anion and Cation Order in Iodide-Containing Mg/Zn-Al Layered Double Hydroxides**

Reproduced with permission from "Laure Aimoz, Christine Taviot-Guého, Sergey V. Churakov, Marina Chukalina, Rainer Dähn, Enzo Curti, Pierre Bordet, and Marika Vespa (2012) Anion and Cation Order in Iodide-Containing Mg/Zn-Al Layered Double Hydroxides. *The Journal of Physical Chemistry C*. 116(9): 5460-5475" Copyright 2012 American Chemical Society.

This article is available on <http://pubs.acs.org/>

## **Chapter 4: Structural Insight into Iodide Uptake by AFm Phases**

Reproduced with permission from “Structural Insight into Iodide Uptake by AFm Phases (2012). Laure Aimoz, Erich Wieland, Christine Taviot-Guého, Rainer Dähn, Marika Vespa, and Sergey Churakov. *Environmental Science & Technology*. DOI: 10.1021/es204470e.” Copyright 2012 American Chemical Society.

This article is available on <http://pubs.acs.org/>

## **Chapter 5: Thermodynamics of AFm-(I<sub>2</sub>, SO<sub>4</sub>) Solid Solution and of its End-Members in Aqueous Media**

“Thermodynamics of AFm-(I<sub>2</sub>, SO<sub>4</sub>) Solid Solution and of its End-Members in Aqueous Media” written by Laure Aimoz, Dmitrii A. Kulik, Erich Wieland, Enzo Curti, Barbara Lothenbach, and Urs Mäder, submitted for publication.



## **Chapter 6: Concluding Remarks and Future Work**

## Concluding Remarks and Future Work

The formation of a solid solution between AFm-SO<sub>4</sub> and AFm-I<sub>2</sub> is a promising mechanism for the immobilization of <sup>129</sup>I in the cementitious barrier of a repository for radioactive waste. Owing to the given sorption isotherms of iodide by AFm-SO<sub>4</sub>, a considerable amount of <sup>129</sup>I is expected to be immobilized in an AFm-SO<sub>4</sub>-rich environment.

The formation of the AFm-I<sub>2</sub> – AFm-SO<sub>4</sub> solid solution also depends on the availability of competing anions, notably carbonate or chloride, which may destabilize the AFm-SO<sub>4</sub> – AFm-I<sub>2</sub> solid solution by formation of AFm-CO<sub>3</sub> and AFm-Cl<sub>2</sub>. Up to now, thermodynamic models of hydrated ordinary Portland cement (OPC) suggest that AFm-SO<sub>4</sub> is not stable in carbonate-rich systems. Further investigations on the stability of solid solutions of AFm phases with multiple end-members, including sulfate and other anions present in cementitious systems, are strongly recommended as they could modify thermodynamic predictions of OPC and reveal the stability of sulfate-containing solid solutions. As a hypothetical example, if Kuzel's salt (an AFm phase containing chloride and sulfate anions) would form a solid solution with AFm-CO<sub>3</sub>; this solid solution may also become a potential phase for the retention of iodide.

Such findings would help in understanding batch sorption experiments, supposedly at equilibrium, where a considerable uptake of iodide onto carbonate-containing hydrated OPC has been measured (Bonhoure, I., et al., 2002. *Radiochim. Acta* **90**, 647-651). In addition, the uptake of iodide by other cement phases like Kuzel's salt (AFm-Cl<sub>2</sub>-SO<sub>4</sub>), AFm-(OH)<sub>2</sub>, and AFm-OH-(CO<sub>3</sub>)<sub>0.5</sub> merits further attention.

Attention to calcium-sulfoaluminate (CSA) cement as a beneficial component of the multi-barrier concept of radioactive waste repository is also encouraged. Indeed, sulfate-containing phases are expected to be stable in CSA cement. Such CSA cement could therefore enhance the retention of many anionic contaminants including <sup>129</sup>I, as long as it remains stable, i.e. as long as it is not destabilized by carbonate, which slowly diffuses into the cementitious barrier.

By assuming the presence of AFm-SO<sub>4</sub> in the cementitious barrier, long-lived radionuclides such as <sup>129</sup>I may be retained by AFm-SO<sub>4</sub> in the near-field as long as the cementitious material remains stable. Eventually, <sup>129</sup>I will be released into the far-field, once portlandite will be consumed by carbonate to form calcite, resulting in a drop of pH and a destabilization of LDH phases. Therefore, another interesting aspect to be further developed, notably for long term predictions, is also the potential stability of LDH phases in the repository far-field for further reducing the predicted <sup>129</sup>I release doses. Even minor quantities of sulfate-containing LDH may still contribute in immobilizing trace levels of <sup>129</sup>I. This phenomenon is not restricted to Ca-Al LDH; for example, the ubiquitous sulfate-containing green rust minerals (Fe<sup>2+</sup>-Fe<sup>3+</sup> LDH, see Figure 1.1) could also be of particular interest.

By highlighting the benefit of LDH phases to incorporate <sup>129</sup>I, this PhD study further encourages additional research work for the other critical anionic radionuclides such as <sup>79</sup>Se (as SeO<sub>3</sub><sup>2-</sup> or also Se<sup>2-</sup> in reducing environments), and also <sup>99</sup>Tc (as TcO<sub>4</sub><sup>-</sup>). Although major advancements in the understanding of LDH crystal chemistry have been made in this thesis, knowledge of solid solution formations was limited to a single species (<sup>129</sup>I) in this PhD work. New similar investigations are required to be performed for other anionic nuclides.

### A guideline for future work

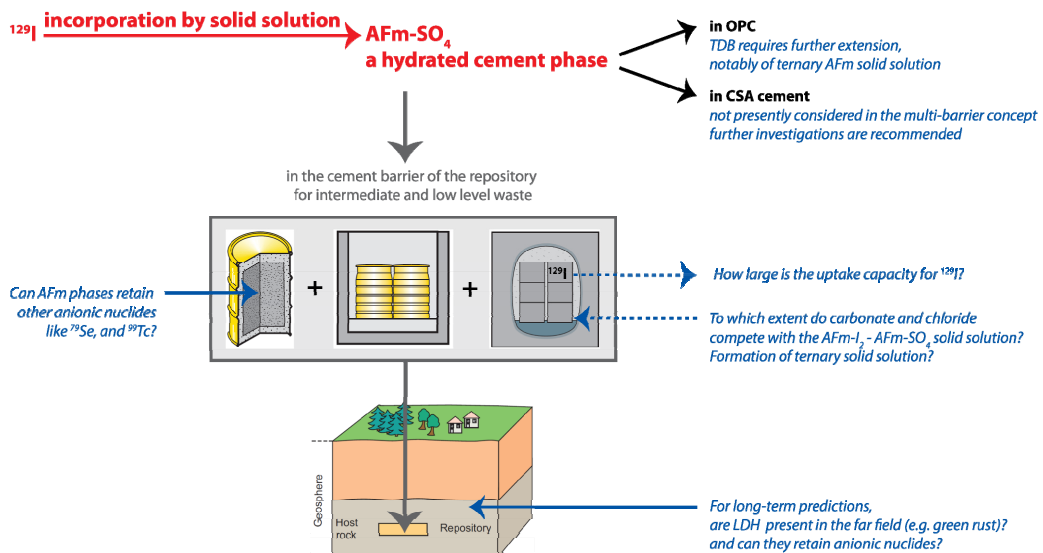


**Figure 6.1.** A guideline for future work. Drawings from Nagra Technical Report. NTB 02-05. Nagra, Wettingen, Switzerland (NAGRA, 2002)

From a technical point of view, special care to solid and liquid phase characterization, especially aiming at a structural understanding at a molecular level of the solid is recommended and essential for developing robust thermodynamic solid solution models for LDH systems. The binding of a given anionic species in a solid solution depends on the crystallographic structure of each end-member, including features like stacking repetition and short-range ordering of anions in the interlayer galleries. The degree of hydration and location of water molecules in the structure plays a key role in building the H-network in LDH, with consequences on the location of anions and on their anionic exchange capacity. Since powder X-ray diffraction techniques are not very effective in locating light elements such as H and O, it is recommended to obtain additional information on the water location using neutron diffraction, for example by synthesizing  $^2\text{H}$ -labelled materials. Furthermore, the increasing power of molecular dynamic simulations will also help in getting a much more precise description of LDH material in terms of structure and dynamics of interlayer species.

In addition, the accuracy and level of complexity of thermodynamic models highly depend on the precision of chemical analysis, especially of the liquid phase in equilibrium with the solids. Application of the Lippmann diagrams or other tools describing solid solutions (e.g. Rozeboom plots) is therefore only recommended when the precision of the chemical analysis is sufficient to obtain a trend between two end-members. Such trends can be well determined owing to reasonable accuracy and precision of chemical analysis and when the difference in the end-member solubility products is sufficiently large. In order to obtain interpretable experimental results it is therefore advised to check the accessible analytical precision well before starting long-lasting and expensive experimental work. In the analytical conditions available for the present work, a difference of 2 *log* units in the solubility product between the two end-members was satisfactory to develop such a model.

Solubility experiments of cement phases can sometimes require long ageing times to reach equilibrium, e.g., the mismatch of solubility products of AFm-I<sub>2</sub> between supersaturation and undersaturation experiments indicates that even after 6 months of equilibration, a true thermodynamic equilibrium was not reached. Therefore, long-term experiments are essential to providing satisfactory thermodynamic data, as well as considering solubility experiments both at supersaturation and undersaturation, allowing to detecting the achievement of equilibrium conditions. This in turn requires a careful planning of the usually restricted time resources in PhD studies.

## Erklärung

Gemäss Art. 28 Abs. 2 RSL 05

**Laure Aimoz**

Matrikelnummer: 08-105-207

Studiengang: Erdwissenschaften

Titel der Arbeit: Structural and Thermodynamic Investigation of Iodide Uptake by Pyrite and Layered Double Hydroxides

Ich erkläre hier, dass ich diese Arbeit selbständig verfasst und keine anderen als die angegebenen Quellen benutzt habe. Alle Stellen, die wörtlich oder sinngemäss aus Quellen entnommen wurden, habe ich als solche gekennzeichnet. Mir ist bekannt, dass andernfalls der Senat gemäss Artikel 36 Absatz 1 Buchstabe o des Gesetzes vom 5. September 1996 über die Universität zum Entzug des auf Grund dieser Arbeit verliehenen Titels berechtigt ist.

Villigen, den 22. Februar 2012

## Curriculum Vitae

### Laure Aimoz

Date of birth: 23.10.82  
 Place of birth: Seoul (South Korea)  
 Nationality: French  
 Contact: laure.aimoz@gmail.com

### Education

2008-2012 Ph.D. degree  
 University of Bern, Institute of Geological Sciences (Switzerland)

2004-2005 M.Sc. degree in environmental analytical chemistry (honors)  
 University College of Cork (Ireland)

2002-2004 Engineering degree (Master's degree level)  
 Ecole Nationale Supérieure des Ingénieurs en Arts Chimiques et Technologiques, Institut National Polytechnique de Toulouse (France)

2000-2002 Cycle Préparatoire Polytechnique of Grenoble (France)  
 A two-year university level course to enter the engineering schools of the French national polytechnic institutes

2000 French high school diploma (Baccalauréat), major in science (honors)

### Work Experience

2008-2012 PhD student  
 Paul Scherrer Institut, Laboratory for Waste Management (Switzerland)  
Thesis: Structural and Thermodynamic Investigation of Iodide Uptake by Pyrite and Layered Double Hydroxides

2006-2008 Research assistant  
 Pacific Centre for Isotopic and Geochemical Research (Vancouver, Canada)  
 Laboratoire d'Océanologie et de Géosciences (Wimereux, France)  
Project: Iron Isotopic Fractionation in Atmospheric Aerosols

2005 Internship  
 Paul Scherrer Institut, Laboratory for Waste Management (Switzerland)  
Project: Synthesis and Characterization of Cement Minerals

2004 Internship  
 Laboratory of Geophysics and Tectonophysics (Grenoble, France)  
Project: Sorption mechanism of arsenic onto iron phosphates

2001-2003 Summer jobs  
 Environmental and occupational health audit in Pechiney group (France)  
 R&D project, recycling of chlorinated waters Métaux Spéciaux (France)  
 Operator in the control laboratory UCAR, graphite producer (France)

## **Publications**

### JOURNAL ARTICLES

**L. Aimoz**, D.A. Kulik, E. Curti, E. Wieland, B. Lothenbach, and U. Mäder. Thermodynamics of AFm-(I<sub>2</sub>,SO<sub>4</sub>) Solid Solution and of its End-Members in Aqueous Media. *Submitted for publication*.

**L. Aimoz**, E. Wieland, C. Taviot-Guého, R. Dähn, M. Glaus, and S.V. Churakov (2012) Structural Insight into Iodide Uptake by AFm phases. *Environmental Science & Technology*. DOI: 10.1021/es204470e.

**L. Aimoz**, C. Taviot-Guého, S.V. Churakov, M. Chukalina, R. Dähn, E. Curti, P. Bordet, and M. Vespa (2012) Anion and Cation Order in Iodide-bearing Zn/Mg-Al Layered Double Hydroxides. *The Journal of Physical Chemistry C*. 116(9): 5460-5475.

**L. Aimoz**, E. Curti, U. Mäder (2011) Iodide interaction with natural pyrite. *Journal of Radioanalytical and Nuclear Chemistry*. 288 (2): 517-524.

P. Flament, N. Mattielli, **L. Aimoz**, M. Choël, K. Deboudt, J. de Jong, J. Rimetz-Planchon, D. Weis (2008) Iron Isotopic Fractionation in Industrial Emissions and Urban Aerosols. *Chemosphere*. 73 (11): 1793-1798.

M. Choël, K. Deboudt, P. Flament, **L. Aimoz**, X. Meriaux (2007) Single-Particle Analysis of Atmospheric Aerosols at Cape Gris-Nez, English Channel: Influence of Steel Works on Iron Apportionment. *Atmospheric Environment*. 41(13): 2820-2830.

### CONFERENCE PROCEEDINGS

**L. Aimoz**, E. Wieland, C. Taviot-Guého, M. Vespa, and R. Dähn. I K-edge EXAFS Spectroscopy of Iodide-Containing AFm Phases. *International Council for Applied Mineralogy, Trondheim, 2011*.

**L. Aimoz**, E. Wieland, D.A. Kulik, B. Lothenbach, M. Glaus, and E. Curti. Characterization and Solubility Determination of the Solid Solution between AFm-I<sub>2</sub> and AFm-SO<sub>4</sub>. *Nuwcem, symposium on cement-based materials for nuclear wastes, Avignon, 2011*.

### CONFERENCE ABSTRACTS

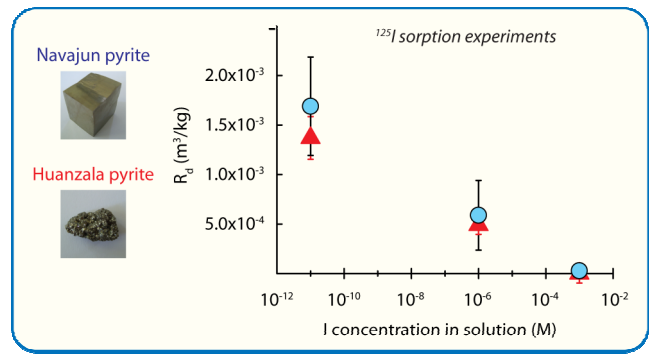
**L. Aimoz**, C. Taviot-Guého, M. Vespa, R. Dähn, U. Mäder, E. Curti. Iodide Uptake by Zn-Al Layered Double Hydroxides. *International Mineralogical Association, Budapest, 2010*.

A. Kitamura, E. Curti, **L. Aimoz** (2009) Reductive Sorption of Se(IV,VI) onto Pyrite: a  $\mu$ -XRF/XAS Study. *Goldschmidt conference, Davos, 2009*.

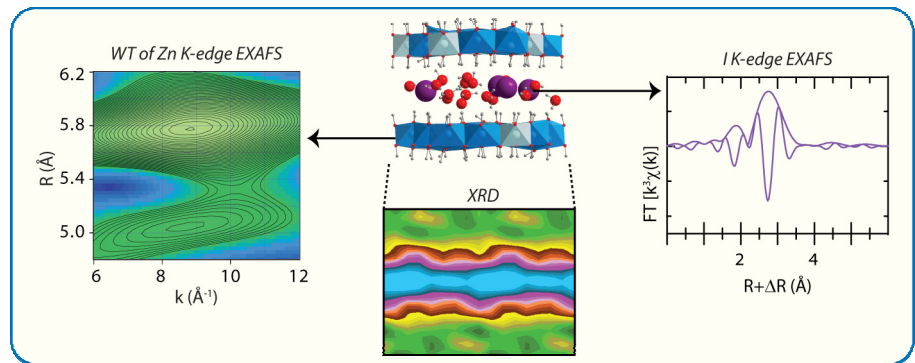
**L. Aimoz**, J. Barling, K. Deboudt, P. Flament, D. Weis (2008) Argide Interference Reduction for Fe Isotopic Analysis by MC-ICP-MS. *Goldschmidt conference, Vancouver, 2008*.

**This PhD thesis aimed at identifying and quantifying potential mechanisms for the retardation of  $^{129}\text{I}$  by sorption and/or incorporation processes onto and into minor minerals relevant for a nuclear waste repository.**

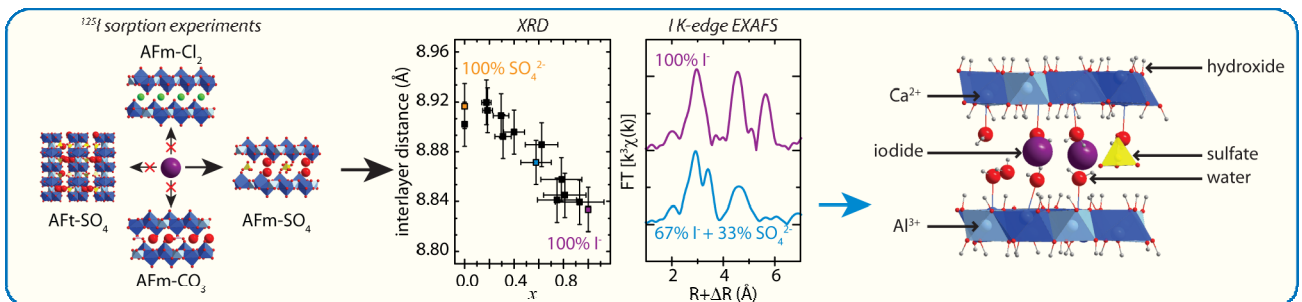
The uptake of iodide ( $\text{I}^-$ ) by natural pyrite was investigated under nearly anoxic conditions ( $\text{O}_2 < 5$  ppm). Our results suggest that iodide uptake was related to the formation of  $\text{Fe(III)}$  oxide clusters at the pyrite surface due to reaction with dissolved oxygen. Thus, pyrite cannot be considered as an effective scavenger of  $^{129}\text{I}$  under the geochemical conditions prevailing in underground radioactive waste geological storage.



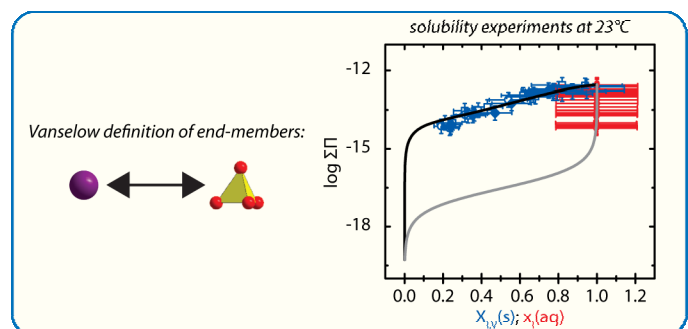
The location of charged centers in  $(\text{Mg}/\text{Zn})_3\text{Al}-\text{I}$  LDH was investigated using techniques sensitive to both short- and long-range order. This study showed that although cations are ordered, interlayer species are not affected and behave as if the cationic layer was charge homogeneous.



The ability of cement phases carrying positively charged surfaces to retard the mobility of  $^{129}\text{I}$  was investigated. This study showed the formation of a solid solution via anion exchange between  $\text{AFm}-\text{I}_2$  and  $\text{AFm}-\text{SO}_4$ , with a short-range mixing of iodide and sulfate. This study further revealed that chloride and carbonate are strong competitors for iodide.



Thermodynamic properties of  $\text{AFm}-\text{I}_2$  and its solid solution with  $\text{AFm}-\text{SO}_4$  were evaluated based on precipitation and dissolution experiments. A satisfactory model was obtained by assuming a subregular solid solution and by using the Vanselow convention for the definition of end-members.



**The formation of a solid solution between  $\text{AFm}-\text{SO}_4$  and  $\text{AFm}-\text{I}_2$  is a promising mechanism for the immobilization of  $^{129}\text{I}$  in the cementitious barrier of a repository for radioactive waste.**